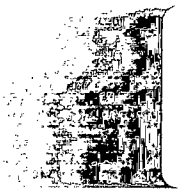

NASA Contractor Report 3777

TWINTN4: A Program for Transonic Four-Wall Interference Assessment in Two-Dimensional Wind Tunnels

William B. Kemp, Jr.

COOPERATIVE AGREEMENT NCC1-69
FEBRUARY 1984

NASA

NASA Contractor Report 3777

TWINTN4: A Program for Transonic Four-Wall Interference Assessment in Two-Dimensional Wind Tunnels

William B. Kemp, Jr.
Virginia Associated Research Campus
Newport News, Virginia

Prepared for
NASA Langley Research Center
under Cooperative Agreement NCC1-69

NASA
National Aeronautics
and Space Administration

Scientific and Technical
Information Office

1984

SUMMARY

A method for assessing the wall interference in transonic two-dimensional wind tunnel tests including the effects of the tunnel sidewall boundary layer has been developed and implemented in a computer program named TWINTN4. The method involves three successive solutions of the transonic small disturbance potential equation to define the wind tunnel flow, the equivalent free air flow around the model, and the perturbation attributable to the model. Required input includes pressure distributions on the model and along the top and bottom tunnel walls which are used as boundary conditions for the wind tunnel flow. The wall-induced perturbation field is determined as the difference between the perturbation in the tunnel flow solution and the perturbation attributable to the model. The methodology used in the program is described and detailed descriptions of the computer program input and output are presented. Input and output for a sample case are given in an appendix.

INTRODUCTION

A transonic computation procedure for assessing the wall interference on an airfoil section tested in a two-dimensional wind tunnel was outlined in reference 1 and described and demonstrated in reference 2. Reference 3 is a user's guide to the computer program TWINTAN in which this procedure is implemented. Measured pressure distributions on the upper and lower tunnel walls and on the airfoil model are used as input and the procedure calculates velocity perturbations over the model due to interference of the upper and lower walls under the assumption that the tunnel flow is two-dimensional.

Barnwell showed in reference 4 that the three-dimensional distortion caused by interaction between the pressure field around the airfoil and the thickness perturbations of the boundary layers on the tunnel side walls was equivalent, under the Prandtl-Glauert similarity rule, to a reduction in Mach number of a two-dimensional flow. Sewall in reference 5 reformulated the sidewall boundary layer effects using the Von Karman transonic similarity rule and showed that his formulation was capable of correlating experimental data obtained with various artificially thickened sidewall boundary layers.

The study of reference 6 identified two alternative procedures for combining the Sewall method of correcting for the sidewall boundary layer effects with the TWINTAN method of assessing the interference arising from the upper and lower walls. In the sequential procedure, the Sewall method is used first to define a transformed flow free of sidewall boundary layer effects which is then assessed by the TWINTAN method to quantify the upper and lower wall effects. In the unified procedure, the existence of sidewall boundary layer effects is recognized in an altered governing equation used in the solution of the wind tunnel flow so that the assessment procedure quantifies the interference effects from all four walls at once. A revised version of the TWINTAN computer program, capable of performing the combined four-wall

interference assessment by either of the two procedures, has been developed and is named TWINTN4. The present paper provides documentation to aid the user of the TWINTN4 program. This paper presents the methodology used in the program and a detailed description of the input required and output provided by the program. The input data is summarized in Appendix A and input and output for a sample case are given in Appendix B.

One significant difference between the two programs should be noted. In the TWINTAN program, the Mach number correction was determined from the local wall-induced velocity perturbation at a user-specified match point location. TWINTN4 does not use a match point. Instead, the corrected Mach number and angle of attack result from minimization of the mean square difference between the surface velocity over the airfoil in the tunnel and that over the same shape airfoil at the same lift in free air. In effect, this procedure is the same as that suggested by Murman in reference 7. In TWINTN4, however, the minimization process is imbedded in and performed simultaneously with the relaxation of the potential solution for the free air case. Thus, the free air pressure distribution which best matches that in the tunnel is found with little additional computation time.

SYMBOLS

a	coefficient of ϕ_y in boundary condition expressions
A,B,C,D	coefficients in tridiagonal form of governing equation
B′,D′	coefficients in line relaxation algorithm
b	half width of tunnel
c	airfoil chord
c_ℓ	section lift coefficient
f	transformation derivative in longitudinal direction
g	transformation derivative in transverse direction
H	nominal shape factor of sidewall boundary layer
j	longitudinal grid index, also longitudinal computational coordinate
k	transverse grid index, also transverse computational coordinate
M	Mach number
n	stretching parameter in coordinate transformation
P,Q	quantities in the finite difference form of the governing equation
q	dynamic pressure

s	distance along airfoil surface
S	term containing sidewall boundary layer properties
U	longitudinal velocity of uniform flow
V	resultant velocity
x	longitudinal physical coordinate
y	transverse physical coordinate
z	general physical coordinate
α	angle of attack
Γ	circulation
γ	ratio of specific heats
Δ	prefix denoting an increment
δ	scaling parameter in coordinate transformation
δ^*	nominal displacement thickness of sidewall boundary layer
ζ	general computational coordinate
Λ	coefficient of longitudinal term in governing equation
μ	switching parameter in finite difference formulation of the governing equation
Φ	total velocity potential
ϕ	dimensionless perturbation velocity potential

Subscripts:

x,y	denote partial differentiation with respect to x or y
j,k	denote value at j-th or k-th grid line
R	reference condition in transformed tunnel flow
T	wind tunnel reference conditions
∞	corrected far field conditions

METHODOLOGY

Wall Interference Assessment Procedure

The procedure implemented in program TWINTN4 involves three successive finite-difference transonic flow solutions. To allow comparison betwen solutions with different values of the far field velocity U_∞ a dimensionless perturbation potential ϕ is defined relative to the total dimensional velocity potential Φ by the relation

$$\Phi = U_R \, c \left(\frac{U_\infty}{U_R} \frac{x}{c} + \phi \right) \tag{1}$$

where U_R is the velocity corresponding to the reference Mach number. This perturbation potential is governed by an extended form of the transonic small disturbance equation expressed as

$$A\phi_{xx} + \phi_{yy} = 0 \tag{2}$$

where

$$A = 1-M_\infty{}^2 + S - (\gamma+1)M_\infty{}^2 \frac{U_R}{U_\infty} \phi_x \left(1 + \frac{U_R}{2U_\infty} \phi_x \right)$$

The tunnel sidewall boundary layer effects are introduced through the term S as discussed in the section headed "Sidewall Boundary Layer". The higher order term in ϕ_x is included to improve the equivalence between changes in ϕ_x and U_∞. The first solution is a calculation of the flow around the test airfoil in the wind tunnel. For this solution U_∞ is set equal to U_R. Pressure distributions measured during the test to be assessed, both on the airfoil and at the upper and lower walls, are imposed as boundary conditions to enhance the fidelity of reproduction of the actual tunnel flow. The assumptions and inaccuracies usually encountered in modeling the ventilated walls and the remaining tunnel geometry are thereby avoided. The airfoil shape defined by this solution is equivalent to the displacement effect of the model plus upper and lower surface boundary layers.

The second solution is a calculation of the free-air flow around this equivalent airfoil shape. As this solution relaxes toward convergence, the angle of attack correction is updated to satisfy the Kutta condition for a lift corresponding to that in the tunnel flow, and the far field velocity and Mach number are updated according to an optimization algorithm which seeks to match the airfoil pressure distribution in free air as closely as possible to that in the tunnel flow. Upon convergence, the correction to angle of attack and the corrected Mach number are immediately available. The measured airfoil pressure coefficients and lift coefficient can now be adjusted to the new reference Mach number and the calculated pressure distribution in free air is available for

comparison. Differences between the two pressure distributions are attributable to higher order interference effects (nonuniformity of the wall-induced velocity field). If these differences are judged small enough to have a negligible effect on the airfoil boundary layer properties, the free air pressure distribution can be considered to be fully corrected for wall interference.

The third solution is another free-air solution at the corrected far field Mach number and is performed to define the flow perturbation attributable to the model. The wall-induced perturbation field is then determined as the difference between the model perturbation and the total perturbation defined by the tunnel flow solution. For this purpose, the model boundary conditions for the third solution are imposed in the form of singularity distributions extracted from the tunnel flow solution. With this model specification the airfoil camber shape is free to be distorted in response to removal of the wall-induced velocity field.

Some features of the method are described in more detail in the following sections to aid the user in adapting the program to a specific facility as well as in making refinements.

Sidewall Boundary Layer

At the option of the user, either a sequential or a unified procedure (see reference 6) is used to account for the sidewall boundary layer. With either option, the sidewall boundary layer effects are embodied in the term S which appears as an increment in the coefficient of the longitudinal term in the governing equation (2). This term is evaluated initially as

$$S = \frac{2\delta^*}{b}\left(2 + \frac{1}{H} - M_T^2\right)$$

The sequential procedure uses the similarity rule developed by Sewall (reference 5) to define an equivalent two-dimensional tunnel flow. The transformed reference Mach number M_R is found by solving

$$\frac{M_R}{(1-M_R^2)^{3/4}} = \frac{M_T}{(1-M_T^2+S)^{3/4}}$$

and all input pressure coefficients and lift and drag coefficients are then transformed by multiplying them by

$$\left(\frac{1-M_T^2+S}{1-M_R^2}\right)^{1/2}$$

The value of S is then set to zero for all of the finite difference solutions.

Under the unified procedure, no similarity transformation is made; instead, the sidewall boundary layer effects are entered into the governing equation used for the tunnel flow solution through the modifying term S, and the reference Mach number M_R is set equal to M_T. The value of S is then set to zero only for the subsequent free-air flow solutions.

Governing Equation

For the numerical solutions, the governing equation (2) is expressed by a conservative form finite difference approximation described by the following expressions:

$$\phi_{yy} = g_k \left[(\phi_y)_{j,k+\frac{1}{2}} - (\phi_y)_{j,k-\frac{1}{2}}\right]$$

$$\Lambda\phi_{xx} = f_j \left[(1-\mu_j)P_j + \mu_{j-1}P_{j-1}\right]$$

$$P_j = \Lambda_j \left[(\phi_x)_{j+\frac{1}{2},k} - (\phi_x)_{j-\frac{1}{2},k}\right]$$

$$\Lambda_j = 1 - M_\infty^2 + S - (\gamma+1)M_\infty^2 \frac{U_R}{U_\infty} Q_j \left(1 + \frac{U_R}{2U_\infty} Q_j\right)$$

$$Q_j = \frac{1}{2}\left[(\phi_x)_{j+\frac{1}{2},k} + (\phi_x)_{j-\frac{1}{2},k}\right]$$

$$\mu_j = \begin{cases} 0 \text{ if } \Lambda_j \geq 0 \\ 1 \text{ if } \Lambda_j < 0 \end{cases}$$

$$f_j = \left(\frac{dj}{dx}\right)_j$$

$$g_k = \left(\frac{d|k|}{dy}\right)_k$$

In defining the transformation derivatives f and g, the quantities j and k each serve the dual role of computational variable and grid index because the transformation is scaled so that the mesh size is one unit of the computational variable. The first derivatives of ϕ appearing in the preceding expressions are all formed by single mesh differencing; for example:

$$(\phi_y)_{j,k+\frac{1}{2}} = g_{k+\frac{1}{2}}(\phi_{j,k+1}-\phi_{j,k})$$

In the following discussion, points in the lower half plane will be identified by a negative sign on the k index. Accordingly, $g_{-k} = -g_k$.

The governing equation is arranged in the tridiagonal form

$$A_k\phi_{j,k-1} + B_k\phi_{j,k} + C_k\phi_{j,k+1} = D_k \tag{3}$$

along j = constant lines and is solved by the method of successive line overrelaxation subject to boundary conditions imposed in Dirichlet form at the outer boundary and in various forms at the airfoil. The development of these boundary conditions for the three flow computations is described in subsequent sections. The implicit algorithm used to solve equation (3) along each line is based on the recursive relationship

$$\phi_{j,k} = D'_k + B'_k\phi_{j,k-1} \tag{4}$$

where the coefficients B' and D' are defined by

$$D'_k = \frac{D_k - C_kD'_{k+1}}{B_k + C_kB'_{k+1}}$$

$$B'_k = \frac{-A_k}{B_k + C_kB'_{k+1}}$$

and are calculated recursively starting with the outer boundary conditions and proceeding inward to $k = \pm 2$.

Because of the symmetric grid indexing used, the $k = 1$ grid line is treated numerically as a boundary along its entire length. At points ahead of the airfoil and in the wake, the boundary condition is derived from the governing equation. In the wake, the potential jump relation

$$\phi_{j,-1} = \phi_{j,1} - \Gamma \tag{5}$$

is used along with equation (4) applied at $k = \pm 2$ to write equation (3) at $k = 1$ and obtain the solution

$$\phi_{j,1} = \frac{D_1-C_1\left[D'_2+D'_{-2} + (1-B'_{-2})\right]}{B_1+C_1(B'_2+B'_{-2})} \tag{6}$$

Equations (5) and (4) are then used to complete the line solution. The same

procedure, but with $\Gamma = 0$, is used ahead of the airfoil.

Boundary Conditions for Tunnel Flow Computation

All input pressure coefficients are interpolated onto the appropriate longitudinal mesh center points, converted to the form of velocity magnitude squared using the exact pressure coefficient definition, and stored in this form. The boundary conditions for the tunnel flow computation are derived primarily from these data.

On the longitudinal outer boundaries at $k = \pm KW$, values of ϕ_x are found from

$$V^2 + (1+\phi_x)^2 + \phi_y{}^2 \quad . \tag{7}$$

and integrated to determine the boundary values of ϕ. Values of ϕ_y are assumed initially to be zero and then are updated iteratively. The ϕ_x gradients approaching the ends of the upper and lower boundaries are used with the governing equation (2) to find ϕ_{yy} at each boundary corner. At the two upstream corners, ϕ_y is specified by input quantities. The variation of ϕ on the upstream boundary is described as a fourth degree polynomial in y whose coefficients are determined from the values of ϕ_y and ϕ_{yy} noted above and the assumption that $\phi = 0$ at the lower upstream corner. On the downstream boundary, ϕ is defined as a cubic in y with the term $\Gamma/2 \operatorname{sgn} y$ added to provide the needed potential jump across the wake. The four coefficients are determined to satisfy the known values of ϕ and ϕ_{yy} at the corners.

The airfoil boundary conditions are imposed in Dirichlet form on a slit at $y = 0$ rather than on the airfoil surface. It is not appropriate to require that the airfoil surface velocities be reproduced on the slit. Instead, we require that the longitudinal distribution of velocity potential on the airfoil surface be reproduced on the slit. Thus,

$$\int V \frac{ds}{dx}\, dx = \int (1+\phi_x)\, dx \tag{8}$$

where V is the airfoil surface velocity determined from the pressure coefficients and ds is the element of surface arc length. The present program calculates ϕ_x by equating the integrands of equation (8) using the approximation

$$\frac{ds}{dx} = (1+\phi_y{}^2)^{\frac{1}{2}}$$

in which ϕ_y is calculated at the slit and is updated iteratively. This procedure may be recognized as an adaptation of the Riegels rule.

The approximations inherent in the above procedure are unacceptable at a blunt leading edge, therefore equation (8) is used to determine ϕ_x for only those mesh intervals downstream of the leading edge. In the mesh interval bracketing the leading edge, upper and lower surface values of ϕ_x are determined such that two broad constraints are satisfied. The first requires that the total circulation determined by integrating $\Delta\phi_x$ over the entire airfoil chord must correspond to the prescribed lift coefficient. The circulation error is corrected directly by adjusting the $\Delta\phi_x$ in the leading edge interval. The second constraint is the airfoil thickness closure condition which requires that the net source strength determined by integrating $\Delta\phi_y$ over the entire airfoil chord must correspond to the prescribed drag coefficient. This constraint is implemented by allowing the error in net source strength to control the average value of ϕ_x in the leading edge interval. The direct effect of negative ϕ_x at the leading edge is to depress the value of ϕ at the first grid point behind the leading edge, thereby creating source strength at this point. As a secondary effect, however, added source strength is created over the entire chord with a distribution such that the ϕ_x boundary conditions are still satisfied in each mesh interval. The existence of such a source distribution which has no effect on ϕ_x anywhere on the chord line causes the thickness design problem to be ill posed without a specific constraint on thickness closure. The role of the thickness closure constraint in the airfoil thickness design problem is analogous to the role of the Kutta condition in the airfoil lift analysis problem.

Solution Process for Equivalent Free-Air Flow Computation

In the equivalent free-air computation, the equivalent airfoil shape determined by the tunnel flow solution is placed in a free-air environment at an angle of attack and Mach number such that the lift is identical with that in the tunnel and the distribution over the airfoil surface of total velocity magnitude is a best fit to that in the tunnel. The free-air environment is established by using outer boundary conditions calculated from a far field analytic expression which includes the two-dimensional lift and thickness terms given in reference 8 and an additional term representing the far field influence of the net source strength at the airfoil.

The airfoil shape is defined by values of ϕ_y evaluated at grid points on the slit representing the airfoil. These values may be expressed in terms of ϕ at surrounding grid points by using a ϕ_{yy} equal to $-\Delta\phi_{xx}$. Using the tridiagonal coefficients of equation (3), the results can be written

$$B_1\phi_{j,1} + C\phi_{j,2} = D_1 - a(\phi_y)_{j,1} \tag{9a}$$

$$B_{-1}\phi_{j,-1}+C\phi_{j,-2} = D_{-1}+a(\phi_y)_{j,-1} \tag{9b}$$

The values of ϕ_y evaluated by these expressions from the tunnel flow solution are combined with an angle of attack correction $\Delta\alpha$ and imposed as the airfoil boundary condition for the equivalent free-air computation in the following form

$$\phi_{j,\pm1} = \frac{D_{\pm1}-CD'_{\pm2} \mp a\left[(\phi_y)_{j,\pm1} - \Delta\alpha\right]}{B_{\pm1}+CB'_{\pm2}} \tag{10}$$

where the upper and lower signs refer to the airfoil upper and lower surfaces, respectively. At each relaxation step of the potential solution, the value of $\Delta\alpha$ is adjusted to drive the potential jump at the trailing edge toward agreement with the specified circulation Γ which is imposed as the potential jump across the wake.

At certain relaxation steps, the far field velocity ratio defined as

$$U_f = \frac{U_\infty}{U_R}$$

is updated in accordance with the following algorithm in which the superscript i designates the relaxation step just completed.

$$\left.\begin{aligned}
U_f^{\,i+1} &= U_f^{\,i} + \Delta U_f^{\,i} \\
\Delta U_f^{\,i} &= \Delta U_f^{\,i-\Delta i}\left(.3-.8\,\frac{\Delta E_U{}^i}{|\Delta E_U{}^i|}\right) \\
\Delta E_U^{\,i} &= E_U^{\,i} - E_U^{\,i-\Delta i} \\
E_U^{\,i} &= \left[\frac{1}{n}\sum_{j=1}^{n}\left(V_j^{\,2}-V_{R,j}^{\,2}\right)\right]^{1/2} \\
V_j &= \frac{\left[U_f^{\,i}+(\phi_x)_j^{\,i}\right]}{1+\dfrac{\left[(\phi_y)_j-\Delta\alpha\right]^i}{U_f^{\,i}}}
\end{aligned}\right\} \tag{11}$$

In this process, the airfoil surface velocity magnitude V is evaluated at each mesh interval on the airfoil slit and the error function E_U is formed as the

root mean square difference between the squares of this velocity distribution and that on which the airfoil boundary condition in the tunnel flow was based (see equation (8)). The interval Δi is the number of iteration steps since the last previous U_f update and depends on the state of relaxation convergence but in no case is less than five.

After each U_f update, the following quantities are evaluated so that the far field boundary conditions and the potential jump across the wake may be updated.

$$\left.\begin{aligned} M_\infty{}^2 &= \frac{U_f{}^2 M_R{}^2}{1+\frac{\gamma-1}{2}M_R{}^2(1-U_f{}^2)} \\ \frac{q_\infty}{q_R} &= \left(\frac{M_\infty}{M_R}\right)^2 \left(\frac{1+\frac{\gamma-1}{2}M_R{}^2}{1+\frac{\gamma-1}{2}M_\infty{}^2}\right)^{\frac{\gamma}{\gamma-1}} \\ \Gamma_\infty &= \Gamma_R U_f \frac{q_R}{q_\infty} \end{aligned}\right\} \quad (12)$$

The velocity ratio is included in the circulation update to account for the fact that Γ (like ϕ) is expressed in units of $U_R c$.

The solution is considered to be converged when both a conventional convergence criterion for the potential relaxation is met and the magnitude of $\Delta E_U/E_U$ has been below a specified level for two successive evaluations of E_U. After convergence, the airfoil pressure distribution in free air is calculated from the airfoil surface velocity magnitudes by the exact C_p equation and the experimental values of lift and pressure coefficients are corrected to the new reference condition by

$$c_{\ell,\infty} = c_{\ell,R}\frac{q_R}{q_\infty} \quad (13)$$

$$C_{p,\infty} = \frac{2}{\gamma}\left(\frac{q_R}{q_\infty M_R{}^2} - \frac{1}{M_\infty{}^2}\right) + C_{p,R}\frac{q_R}{q_\infty} \quad (14)$$

The first term in equation (14) represents the change in free-stream static pressure under the assumption of constant total pressure.

If the unified option for tunnel sidewall boundary layer was selected, equations (13) and (14) correct the coefficients from the tunnel test for interference from all four walls. Under the sequential option, however, the

coefficients had already been adjusted by the similarity rule for sidewall boundary layer and equations (13) and (14) then provide the additional correction for the upper and lower wall effects.

Boundary Conditions for Model Perturbation Computation

The purpose of the model perturbation computation is to define that part of the tunnel flow perturbation which is attributable directly to the airfoil. Accordingly, the airfoil boundary condition in this computation should assure that the vorticity and source distributions on the slit representing the airfoil duplicate those existing in the tunnel flow solution. Thus, the quantities

$$\Delta\phi_j = \phi_{j,1} - \phi_{j,-1} \tag{15a}$$

$$(\Delta\phi_y)_j = (\phi_y)_{j,1} - (\phi_y)_{j,-1} \tag{15b}$$

as extracted from the tunnel flow solution are to be reproduced in the free air computation. From equations (15), (9) and (4) we find

$$\phi_{j,1} = \frac{D_1+D_{-1} - C(D'_2+D'_{-2}) + (B_{-1}+ CB'_{-2})\Delta\phi_j - a(\Delta\phi_y)_j}{B_1 + B_{-1} + C(B'_2+B'_{-2})} \tag{16}$$

which is used along with equation (15a) to impose the airfoil boundary conditions in the model perturbation computation.

In order that the calculated model perturbation represent as closely as possible the perturbation attributable to the model in the tunnel flow solution, it is important, because of the nonlinear governing equation, that the total Mach number environment for the calculation be similar to that in the tunnel. To this end, the far field Mach number used for the model perturbation calculation is that determined during the equivalent free-air solution so that the far field Mach number correction will replace, at least to first order, the Mach number perturbation attributable to the walls in the tunnel flow solution. The free-air outer boundary conditions imposed are also the same as those used in the equivalent free-air solution.

After convergence, the distribution on the tunnel axis of the wall-induced velocities are found by subtracting the model perturbation from the total perturbation calculated in the tunnel flow solution.

DESCRIPTION OF INPUT

Program TWINTN4 is written in FORTRAN 4 and has been implemented on the CDC CYBER 175 computer with a central memory requirement of approximately 70,000 (octal) 60-bit words. The program input is provided in two namelist blocks.

The first, labeled NPUT, contains 12 parameters to define the computational grid, 8 parameters for problem constraint and 8 parameters for numerical process control. The second block, RDPX, provides arrays of wall and model pressure coefficients and their longitudinal locations. All input data are nondimensional with the airfoil chord assumed to be the unit of length. The input parameters are summarized in Appendix A and are discussed in more detail in the following sections.

The program calls several subroutines from the Langley Research Center graphics library to create a plot vector file which can then be post-processed to obtain plotted output. Some modifications to the program might be required to obtain plots on a different computer system.

Computational Grid Inputs

The perturbation potential is stored by the program in an array addressed as PHI(J, K, L). The index L takes on values of 1 or 2 for the upper or lower half plane respectively. J and K are the longitudinal and lateral indices respectively in each half plane. The physical configuration of the upper half grid is sketched in figure 1. The $K = 1$ grid line is the axis of grid symmetry between the two half planes and represents the tunnel center line, $y = 0$. The lower half grid is a mirror image of the upper. The longitudinal grid spacing is uniform from J1 to J4. The longitudinal spacing upstream from J1 and downstream from J4 and the lateral spacing of the entire grid are stretched by transformations of the form

$$z = n\delta \frac{\zeta}{n-\zeta} \tag{17}$$

where z represents a physical coordinate and ζ is the computational coordinate in the corresponding direction. In the present program, the transformation is truncated to prevent z reaching infinity. Equation (17) is used to relate the coordinate x or y directly to the grid index J or K by assuming a computational mesh interval $\Delta\zeta$ of unity. The stretching parameter n then represents the number of mesh intervals which would cover the range $0 \leq z \leq \infty$, and the scaling parameter δ is the limit as z approaches zero of the physical mesh interval Δz. The specific relations for the upstream, downstream and lateral transformations are formed by substituting the parameters tabulated below into equation (17).

Index Range	$1 \leq J \leq J1$	$J4 \leq J \leq J5$	$1 \leq K \leq KB$
ζ	J1 - J	J - J4	K - 1
z	x(J1) - x	x - x(J4)	y
n	M	M	N
δ	DXMN	DXMN	DYMN

The program sets the uniform mesh interval Δx in the range from J1 to J4 equal to DXMN, locates J3 at the airfoil trailing edge (x = 1), and determines J2 such that the airfoil leading edge (x = 0) lies in the mesh space between J2 and J2 + 1. The boundaries of the uniform longitudinal mesh region are

$$X(J1) = 1. - DXMN * (J3 - J1)$$

$$X(J4) = 1. + DXMN * (J4 - J3)$$

The foregoing information is sufficient to determine the physical coordinates x,y of each grid intersection J,K in terms of the following program input parameters. The longitudinal grid used in the free-air computation is defined by the integers J1, J3, J4, J5 and M and the real constant DXMN which must satisfy the following constraints.

$$J5 \leq 100$$

$$J1 \leq M$$

$$J5 - J4 < M$$

$$(J3 - J1) * DXMN \geq 1.$$

$$J4 > J3$$

The grid lines serving as the upstream and downstream boundaries of the tunnel flow computation are denoted by the integers JU and JD respectively which must satisfy:

$$JU \geq 1$$

$$JD \leq J5$$

In addition, all wall boundary points, located at mesh centers from x(JU + 1/2) to x(JD - 1/2) must lie within the longitudinal range of the input wall pressures.

The lateral grid is defined by the integers KB, N and KW and the real constant DYMN which must satisfy:

$$KB \leq 50$$

$$KB \leq N$$

$$KW \leq KB$$

KW identifies the lateral boundary of the tunnel flow computation and must be selected along with N and DYMN such that y(KW) is the lateral distance from the tunnel center line to the upper or lower line of input wall pressures.

The following points should be considered also in selecting grid input parameters. The outer boundaries of the free-air computation, x(1), x(J5) and

y(KB) should lie several chord lengths from the model for best accuracy of the free-air boundary conditions. If, however, J1 and (J5 - J4) closely approach M, and KB closely approaches N, the solution convergence rate is adversely affected.

Problem Constraint Inputs

Seven real and one integer input parameters provide constraints needed in the tunnel flow computation. AMREF is the reference Mach number corresponding to the tunnel reference conditions used in reducing the input data to coefficient form. The lift coefficient CL defines the total airfoil circulation. The accuracy of the calculated wall-induced upwash depends on the accuracy of the CL input. CD is the airfoil drag coefficient which provides the airfoil thickness closure constraint.

The parameters SLA and SLB are the onset flow streamline slopes at the upper and lower corners respectively of the upstream boundary of the tunnel flow computation x(JU). The present formulation presumes that this upstream boundary is located in the solid nozzle region of the tunnel where the flow direction is constrained by the known wall slopes SLA and SLB. If this condition cannot be met or if other conditions, such as poor resolution of the wall pressures prevent accurate modeling of this upstream region, SLA and SLB may be input as zero and the tunnel flow direction monitored by comparing the orientation of the airfoil shape calculated in the tunnel flow solution with the known incidence of the test airfoil. Nominal properties of the tunnel sidewall boundary layer at the model location are input through DSTOB2 which is the displacement thickness divided by the tunnel half width, and H the shape factor. Default values of 0. and 1. respectively are provided for these two parameters and define the case of no sidewall boundary layer.

The integer parameter ISEQ, if set to 1 invokes the sequential procedure for accounting for the tunnel sidewall boundary layer. The default value of zero results in the unified procedure being followed.

Computational Control Inputs

The parameters discussed in this section affect the generation of a plot vector file, and the convergence rate, stabilization, termination and amount of diagnostic output for the iterative process in each of the three solutions. Default values of each of these parameters are established in the program but may be overridden simply by including new values in the NPUT namelist.

The integer parameter IPLOT, if set to 1 causes generation of a plot vector file. The default value of 0 bypasses this feature. The two real parameters RFA and EPSU are used only in the equivalent free air solution. RFA is the feedback gain determining the angle of attack response to a circulation mismatch. EPSU specifies the convergence limit for the far field velocity update.

The five remaining parameters are dimensioned quantities denoting values stored in three-element arrays. The array subscripts from 1 to 3 correspond to the three successive flow solutions. The real array ORF contains the overrelaxation factor used at subsonic points in the successive line overrelaxation procedure. The real array DXT contains a damping factor to retard updating of longitudinal velocity perturbations. The real array EPS contains the convergence criterion in terms of the absolute value of the perturbation potential change in one iteration at the grid location where this change is greatest. Iteration is terminated either when this criterion is met or when the number of iteration steps exceeds the value obtained from the integer array IMX. Information describing the convergence history is available for output at each step of iteration. The values stored in the integer array ITRC determine how much of this information is actually printed. An ITRC value of 1 causes printing at each iteration step; a value of 2 causes printing every tenth step and at termination; and the default value of zero causes only the final values to be printed so that it may be determined whether the iteration converged or ran the maximum number of steps. If either of the first two solutions is terminated by reaching the maximum number of iterations and the final value of the convergence parameter is greater than 10 times the criterion given in EPS, then all further processing of that case is aborted.

Pressure Distribution Inputs

In the tunnel flow computation, the outer boundary conditions are established from the input pressure coefficient distributions along or near the upper and lower tunnel walls. Similarly, the inner boundary conditions are established from input pressure coefficient distributions on the airfoil upper and lower surfaces. These data are input through parameters in the namelist block RDPX. The wall pressure data are described in a two-element integer array and two real two-dimensional arrays. The integers NW(1) and NW(2) are the numbers of pressure input locations along the upper and lower walls respectively. The first real array XW inputs the x coordinates of the wall pressure locations in order from upstream to downstream. The first index numbers these locations from 1 to the appropriate NW element and the second index is 1 or 2 for the upper or lower wall respectively. The second real array CPW inputs the pressure coefficients with the same order and indexing as their corresponding locations. The airfoil upper and lower surface pressure coefficients and their chordwise locations are input in a fully analogous manner using the integers NM(1), and NM(2) and the arrays XM and CPM. All four real arrays are dimensioned to accommodate values of NW or NM up to 30.

All input pressure distributions are interpolated onto boundary points located at the centers of the longitudinal mesh intervals. These boundary points range from J2 + 3/2 to J3 - 1/2 on the airfoil (K = 1) and from JU + 1/2 to JD - 1/2 on the outer boundary (K = KW). The interpolation routine fits a spline to each distribution with a zero second derivative condition at the spline ends. Because the routine as presently implemented does not provide for extrapolation, each input pressure distribution must cover the full range of boundary points Manual extrapolation of the experimental pressures at the airfoil trailing edge might be necessary in some cases to provide the required range of data. Near the leading edge, on the other hand, the number of

experimental measurements might far exceed the requirements of this program and, therefore, one might omit some of the experimental data. Care should be taken not to introduce spurious oscillations in the spline fit between data points. One might even input a false pressure coefficient at the leading edge to help the spline provide a smooth fairing in the range of interest.

DESCRIPTION OF OUTPUT

Output is generated during each major phase of computation so that the user may scrutinize the processes leading to the final wall-induced perturbation results. The process output will be described in four sequential phases, input processing, tunnel flow solution, equivalent free air solution and model perturbation solution. All output velocities are expressed in units of the reference stream velocity corresponding to the input tunnel Mach number AMREF. All output velocity potentials are expressed in units of the product of this reference velocity and the airfoil chord.

Input Processing

The contents of the namelist block NPUT are listed first. If the sequential option has been selected, the sidewall boundary layer similarity transformation is performed prior to all output. The transformed values of AMREF, CL and CD therefore appear in the NPUT listing. The longitudinal grid structure is next described by listing the x location and the derivative dJ/dx. These quantities evaluated at the grid lines J are identified as X(J) and F1(J). The corresponding quantities evaluated at J + 1/2 are given by XMID(J) and F2(J). The lateral grid structure is described by the grid line location Y(K), and the derivative dK/dy evaluated at the grid lines G1(K) and at the K + 1/2 points G2(K). The user should check to see that Y(KW) is the lateral location of the input wall pressures. The results of interpolating the airfoil pressure coefficients onto the mesh midpoints XMID(J) are then listed in separate groups for the upper and lower surfaces. This listing can be used in conjunction with the input data to judge the quality of the spline fit.

Tunnel Flow Solution

The convergence history of the tunnel flow solution is shown by listing the iteration number I, the largest change in the perturbation potential from the previous iteration DPHIMX, and the grid intersection JMX, KMX where this change is located. Negative values of KMX indicate points in the lower half plane. The flag ISUP is 1 if this grid point is a supersonic point and 0 if it is subsonic. The number of supersonic points NS and the current value of airfoil trailing edge thickness TTE are also listed. Both the inner and the outer boundary conditions depend on the solution and therefore are updated iteratively. To avoid using poorly developed data for the update, it is performed only when the convergence parameter DPHIMX is less than some threshold value. The threshold levels specified for the inner and outer boundary condition updates are 10^{-3} and EPS(1)*10 respectively. The threshold levels are separated so that numerical problems associated with each update process might

be identified more readily. Because the initial approximation to the inner boundary conditions is poor, it is normal for the convergence history to show that DPHIMX bounces up from the 10^{-3} level several times before sinking through it. This listing will end either with DPHIMX $\leq$ EPS(1) or with I = IMX(1) depending on whether or not convergence was achieved.

The data in the following listings are identified by a heading as pertinent to the tunnel flow. The critical pressure coefficient is given as CPSTAR. Data evaluated at the airfoil surface are listed next. Two lines are printed for each grid index J. Data on the first line pertain to the upper surface or both surfaces and those on the second line to the lower surface or the increment between surfaces. The first four columns give data evaluated at the center of the mesh interval upstream from J. The calculated shape of the airfoil surface streamlines is given by the coordinates X(J-.5) and YMOD. The pressure coefficient CP(REF) can be compared with the previous listing of interpolated pressure coefficients to see how well the inner boundary conditions were satisfied. The longitudinal perturbation velocity component U is obtained directly from the potential gradient along the K = 1 grid line. The data in the last four columns are evaluated at the grid points located at X(J). V is the lateral component of perturbation velocity and DELTA PHI and DELTA V are the increments between the upper and lower surface values of the perturbation potential and the lateral velocity respectively. These increments are stored for use as model boundary conditions in the model perturbation computation.

The perturbation velocity components along the outer boundaries of the tunnel flow computational region are given next. The first listing pertains to the upstream and downstream boundaries. The different coordinate locations given for the two components reflect the fact that U is evaluated at lateral grid lines and at midpoints in the longitudinal direction while the V component is evaluated at longitudinal grid lines and at midpoints in the lateral direction. In the case of the upper and lower boundaries listed next, the V component is extrapolated to grid points on the K = KW boundary. Thus, the listed values of U and V are given at the indicated longitudinal location along the upper and lower boundaries at K = KW.

The final listing from the tunnel flow solution gives the perturbation potential at grid points in the immediate vicinity of the airfoil. The grid points are those on the K = 1, 2, and 3 grid lines in the upper and lower half planes for J from J1 to J4.

Equivalent Free Air Solution

Data output listed for the equivalent free-air solution is structured similarly to that described for the tunnel flow solution. This discussion, therefore, will highlight the differences between the two.

In the equivalent free-air solution, the angle of attack correction DA is updated after each iteration for which the convergence parameter DPHIMX is less than 10^{-3}. The far field velocity ratio UFAC is updated either as DPHIMX decreases through EPS(2)*10 or if DPHIMX is less than EPS(2) provided five

iterations have occurred since the previous update. The convergence history listing includes the values of DA, UFAC and the error function EU.

After convergence, the final far field Mach number is given as AMINF, the corresponding velocity ratio as UINF/UREF, the dynamic pressure ratio as QFAC, and the angle of attack correction is listed in radians. This far field condition represents the corrected reference condition for the tunnel data. Accordingly, the model surface pressures listed as CP(INF) as well as the critical pressure CPSTAR are in the form of pressure coefficients based on the corrected reference condition. It should be noted that the perturbation velocities listed in the free-air solution output are perturbations from a uniform flow at the far field velocity UINF. The velocity unit, however, is still the tunnel reference velocity or the similarity transformed velocity UREF.

The experimental lift and pressure coefficients, corrected to the new reference condition, are then listed. The pressure coefficients are listed first at the computational mesh centers and then at the original input orifice locations. The root mean square increment between the calculated free air values and the corrected experimental values at mesh centers is given as a measure of the higher order interference effects not accounted for by the corrections to Mach number and angle of attack.

Model Perturbation Solution

The model perturbation solution is a simple potential relaxation with no boundary condition updates. The convergence history is simplified accordingly. After convergence, the flow properties at the airfoil surface are listed in the same form used for the previous solutions.

The wall-induced velocities are calculated as the difference between the perturbation velocities calculated at the same locations in the tunnel flow solution and in this solution. This is performed in the present program only along the tunnel center line (K = 1) from JU to JD. The lateral velocities in the free air solution VF and due to the walls VW are listed at the grid point locations XV. The longitudinal velocity perturbations in the free air solution UF and due to the walls UW are given at the mesh center location XU. Over the model chord, values corresponding to both upper and lower surfaces are given. Although the wall-induced velocities should be identical on the two surfaces, some differences can appear in VW which reflect the accuracy with which the velocity jump boundary condition is satisfied.

The final listing gives the mean of the wall-induced velocity components VW and UW evaluated over the model chord and the standard deviation over the model of these two components and their resultant.

Plotted Output

Two frames of plotted output are generated. In the first frame, the two components of wall-induced velocity are plotted against distance along the tunnel axis extending from about one chord length upstream of the leading edge

to about one chord length downstream of the trailing edge. The longitudinal component is plotted with + symbols and the lateral component with x symbols. The corrected far-field velocity ratio (relative to unity) is plotted with a large + at mid-chord and the angle-of-attack correction is shown by a large x at the trailing edge. The figure title includes the case title (first line of input), the standard deviations over the model of the longitudinal, lateral and resultant wall-induced velocities and information identifying the computer run, date and time.

The second frame compares the corrected experimental airfoil pressure distribution, plotted with asterisks, with the calculated free-air pressure distribution, plotted with + symbols for the upper surface and x symbols for the lower surface. The most upstream points on the calculated curves are plotted at the center of the mesh interval bracketing the leading edge which, of course, might lie upstream of the actual leading-edge location. The critical pressure coefficient is shown by the large + symbol superimposed on the CP scale and the stagnation pressure coefficient is shown by the large x at the leading edge. The figure title includes the corrected values of Mach number and lift coefficient and the rms difference between the calculated and experimental pressure distributions.

APPENDIX A

SUMMARY OF PROGRAM INPUT

TITLE - Title of case. Up to 80 alphanumeric characters to appear in output listing and plotted figure titles.

Parameters in Namelist NPUT

J1 - Longitudinal grid index at beginning of uniform grid spacing.

J3 - Longitudinal grid index at airfoil trailing edge.

J4 - Longitudinal grid index at end of uniform grid spacing.

J5 - Grid index at downstream end of free-air domain.

M - Longitudinal grid spacing in uniform region.

DXMN - Longitudinal grid spacing in uniform region.

JU - Grid index at upstream end of tunnel flow domain.

JD - Grid index at downstream end of tunnel flow domain.

KB - Lateral grid indes at outer edge of free-air domain.

N - Lateral grid stretching parameter.

DYMN - Inner limit value of lateral grid spacing.

KW - Lateral grid index at outer edge of tunnel domain.

AMREF - Tunnel reference Mach number.

CL - Airfoil section lift coefficient.

CD - Section drag coefficient used to define trailing edge thickness.

SLA - Slope of upper tunnel wall at upstream end of tunnel domain.

DSTOB2 - Nominal sidewall boundary layer displacement thickness divided by tunnel width. (Default value = 0.)

H - Nominal sidewall boundary layer shape factor. (Default value = 1.)

ISEQ - Selector for sidewall boundary layer accounting method.
= 0 for unified procedure. (Default value)
= 1 for sequential procedure.

IPLOT - Selector for plot output.
= 0 for no plot vector file. (Default value)
= 1 to generate plot vector file.

RFA - Feedback gain for angle-of-attack correction. (Default value = 0.5)

ORF(I) - Overrelaxation factor for subsonic points in the I-th solution. (Default values = 1.8, 1.8, 1.8)

DXT(I) - Longitudinal velocity update damping factor in the I-th solution. (Default values = 0.5, 0.5, 0.5)

ITRC(I) - Selector for convergence history output.
= 0 for final values only. (Default value for all three solutions)
= 1 for output at each iteration step.
= 2 for output at each tenth step plus final values.

IMX(I) - Maximum number of iteration steps allowed in I-th solution. (Default values = 350, 600, 200)

EPS(I) - Convergence criterion for potential relaxation in I-th solution. (Default values = 10^{-6}, 10^{-5}, 10^{-6})

EPSU - Convergence criterion for far field velocity update. (Default value = 10^{-4})

Parameters in Namelist RDPX

NW(I) - Number of pressure input locations on I-th wall.
I = 1 for upper wall.
I = 2 for lower wall.

XW(J,I) - Array of longitudinal locations for pressure input on I-th wall, J varies from 1 to NW(I).

CPW(J,I)- Array of input pressure coefficients on I-th wall, J varies from 1 to NW(I).

NM(I) - Number of pressure input locations on I-th airfoil surface.
I = 1 for upper surface.
I = 2 for lower surface.

XM(J,I) - Array of longitudinal locations for pressure input on I-th airfoil surface, J varies from 1 to NM(I).

CPM(J,I)- Array of input pressure coefficients on I-th airfoil surface, J varies from 1 to NM(I).

APPENDIX B

SAMPLE CASE

The sample case consists of the application of program TWINTN4 to results from a test of a NACA 0012 airfoil model in the Langley 0.3m Transonic Cryogenic Tunnel with slotted top and bottom walls. The ratio of tunnel height to airfoil chord was 4. The airfoil was set at 2.025° incidence and tested at a reference Mach number of 0.701 and a Reynolds number of 3.05×10^{6}.

The sequential option for accounting for the sidewall boundary layer was chosen for the sample case. The input card images are listed and followed by the program output listing. The plotted output is shown in figures 2 and 3. Figures 4 and 5 show the plotted output from the same case but using the unified procedure for accounting for the sidewall boundary layer.

INPUT FOR SAMPLE CASE

```
NACA 0012, M=.701, ALPHA=2.025, RN=3.046E+06.
 $NPUT J1=25,J3=47,J4=49,J5=73,M=35,DXMN=.0499,
      JU=1,JD=72,KB=22,N=30,DYMN=.05098,KW=18,
      SLA=0.,SLB=0.,DRF(1)=2*1.80,ITRC(1)=2,1,2,
      IMX(1)=350,500,200,IPLOT=1,ISEQ=1,
      AMREF= .701,CL= .2204,CD= .0076,H=1.5042,DSTOR2= 1.543E-02,$
 $RDPX  NM(1)= 24, 24,NW(1)= 26, 28,
  XW(1, 1)= -.40567E+01,
 -.37233E+01, -.33900E+01, -.30567E+01, -.27233E+01, -.23900E+01, -.20567E+01,
 -.17233E+01, -.13900E+01, -.10567E+01, -.72333E+00, -.39000E+00, -.56667E-01,
  .27667E+00,  .61000E+00,  .94333E+00,  .12767E+01,  .16100E+01,  .19433E+01,
  .22767E+01,  .26100E+01,  .29433E+01,  .32767E+01,  .36100E+01,  .39433E+01,
  .42767E+01,
  CPW(1,1)= -.54861E-02,
 -.12283E-02, -.98122E-03,  .62431E-03, -.52061E-03,  .86244E-03,  .11078E-03,
  .13516E-02, -.37153E-02, -.84227E-02, -.19627E-01, -.36989E-01, -.48082E-01,
 -.60229E-01, -.59275E-01, -.50005E-01, -.50088E-01, -.32147E-01, -.33204E-01,
 -.28056E-01, -.32320E-01, -.36963E-01, -.37117E-01, -.36747E-01, -.39867E-01,
 -.39552E-01,
  XW(1, 2)= -.40567E+01,
 -.37233E+01, -.33900E+01, -.30567E+01, -.27233E+01, -.20567E+01, -.17233E+01,
 -.13900E+01, -.10567E+01, -.72333E+00, -.39000E+00, -.56667E-01,  .27667E+00,
  .61000E+00,  .94333E+00,  .12767E+01,  .16100E+01,  .20067E+01,  .23400E+01,
  .26733E+01,  .30067E+01,  .33400E+01,  .36733E+01,  .38400E+01,  .41733E+01,
  .45067E+01,  .48400E+01,  .51733E+01,
  CPW(1,2)= -.22372E-01,
  .69173E-03, -.35306E-02,  .47236E-02,  .14234E-01,  .98306E-02,  .13424E-01,
  .22097E-01,  .18123E-01,  .22969E-01,  .97888E-02, -.56598E-02,  .21510E-02,
  .20283E-03,  .14175E-02,  .84934E-03, -.88307E-03, -.23261E-02, -.70418E-02,
 -.92554E-02, -.15335E-01, -.16095E-01, -.18531E-01, -.18062E-01, -.18691E-01,
 -.18373E-01, -.17930E-01, -.45142E-01,
  XM(1, 1)=  .22477E-03,
  .14361E-01,  .28221E-01,  .52970E-01,  .77977E-01,  .10296E+00,  .15231E+00,
  .20155E+00,  .25228E+00,  .30200E+00,  .35197E+00,  .40145E+00,  .45146E+00,
  .50149E+00,  .55082E+00,  .60089E+00,  .65075E+00,  .70067E+00,  .74982E+00,
  .80091E+00,  .85039E+00,  .89945E+00,  .94878E+00, .987503 ,
  CPM(1, 1)=  .10741E+01,
 -.32689E+00, -.61743E+00, -.83530E+00, -.92300E+00, -.97980E+00, -.94881E+00,
 -.84726E+00, -.70543E+00, -.60428E+00, -.53857E+00, -.48697E+00, -.42540E+00,
 -.37318E+00, -.31092E+00, -.26626E+00, -.22483E+00, -.17602E+00, -.12971E+00,
 -.74062E-01, -.20218E-01,  .44718E-01,  .12041E+00, .21364 ,
  XM(1, 2)=  .22477E-03,
  .11718E-01,  .24341E-01,  .49936E-01,  .74166E-01,  .98549E-01,  .14860E+00,
  .19846E+00,  .24811E+00,  .29807E+00,  .34861E+00,  .39795E+00,  .44826E+00,
  .49806E+00,  .54869E+00,  .59798E+00,  .64853E+00,  .69885E+00,  .74836E+00,
  .79859E+00,  .84924E+00,  .89914E+00,  .94766E+00, .987503 ,
  CPM(1, 2)=  .10741E+01,
  .49190E+00,  .17864E+00, -.10019E+00, -.21237E+00, -.29413E+00, -.36746E+00,
 -.38417E+00, -.37348E+00, -.34969E+00, -.32701E+00, -.30194E+00, -.26462E+00,
 -.23905E+00, -.20599E+00, -.17514E+00, -.15402E+00, -.11758E+00, -.85763E-01,
 -.40814E-01, -.83148E-02,  .29585E-01,  .11052E+00, .255044 ,
 $END
```

SAMPLE CASE OUTPUT

```
$NPUT
J1       = 25,
J3       = 47,
J4       = 49,
J5       = 73,
M        = 35,
DXMN     = .499E-01,
JU       = 1,
JD       = 72,
KB       = 22,
N        = 30,
DYMN     = .5098E-01,
KW       = 18,
AMREF    = .68711860072509E+00,
CL       = .22335850000608E+00,
CD       = .77020172415889E-02,
SLA      = 0.0,
SLB      = 0.0,
RFA      = .5E+00,
ORF      = .18E+01, .18E+01, .18E+01,
DXT      = .5E+00, .5E+00, .5E+00,
ITRC     = 2, 1, 2,
EPS      = .1E-05, .1E-04, .1E-05,
IMX      = 350, 500, 200,
EPSU     = .1E-03,
ISEQ     = 1,
DSTOB2   = .1543E-01,
H        = .15042E+01,
IPLOT    = 1,
```

NACA 0012, M=.701, ALPHA=2.025, RN=3.046E+06.

J	X(J)	F1(J)	F2(J)	XMID(J)
1	-.39083E+01	.19795E+01	.21635E+01	-.36772E+01
2	-.34453E+01	.23557E+01	.25561E+01	-.32497E+01
3	-.30534E+01	.27647E+01	.29815E+01	-.28857E+01
4	-.27176E+01	.32064E+01	.34395E+01	-.25722E+01
5	-.24265E+01	.36808E+01	.39303E+01	-.22993E+01
6	-.21718E+01	.41880E+01	.44538E+01	-.20595E+01
7	-.19470E+01	.47278E+01	.50100E+01	-.18472E+01
8	-.17473E+01	.53004E+01	.55990E+01	-.16580E+01
9	-.15685E+01	.59057E+01	.62206E+01	-.14882E+01
10	-.14077E+01	.65437E+01	.68750E+01	-.13349E+01
11	-.12621E+01	.72144E+01	.75621E+01	-.11960E+01
12	-.11298E+01	.79179E+01	.82819E+01	-.10694E+01
13	-.10090E+01	.86540E+01	.90344E+01	-.95367E+00
14	-.89828E+00	.94229E+01	.98196E+01	-.84736E+00
15	-.79640E+00	.10225E+02	.10638E+02	-.74940E+00
16	-.70236E+00	.11059E+02	.11488E+02	-.65884E+00
17	-.61528E+00	.11926E+02	.12372E+02	-.57487E+00
18	-.53443E+00	.12826E+02	.13288E+02	-.49680E+00
19	-.45914E+00	.13758E+02	.14237E+02	-.42402E+00
20	-.38886E+00	.14723E+02	.15218E+02	-.35603E+00
21	-.32315E+00	.15721E+02	.16232E+02	-.29235E+00
22	-.26153E+00	.16752E+02	.17279E+02	-.23260E+00
23	-.20365E+00	.17815E+02	.18359E+02	-.17641E+00
24	-.14917E+00	.18911E+02	.19472E+02	-.12349E+00
25	-.97800E-01	.20040E+02	.20040E+02	-.72850E-01
26	-.47900E-01	.20040E+02	.20040E+02	-.22950E-01
27	.20000E-02	.20040E+02	.20040E+02	.26950E-01
28	.51900E-01	.20040E+02	.20040E+02	.76850E-01
29	.10180E+00	.20040E+02	.20040E+02	.12675E+00
30	.15170E+00	.20040E+02	.20040E+02	.17665E+00
31	.20160E+00	.20040E+02	.20040E+02	.22655E+00
32	.25150E+00	.20040E+02	.20040E+02	.27645E+00
33	.30140E+00	.20040E+02	.20040E+02	.32635E+00
34	.35130E+00	.20040E+02	.20040E+02	.37625E+00
35	.40120E+00	.20040E+02	.20040E+02	.42615E+00
36	.45110E+00	.20040E+02	.20040E+02	.47605E+00
37	.50100E+00	.20040E+02	.20040E+02	.52595E+00
38	.55090E+00	.20040E+02	.20040E+02	.57585E+00
39	.60080E+00	.20040E+02	.20040E+02	.62575E+00
40	.65070E+00	.20040E+02	.20040E+02	.67565E+00
41	.70060E+00	.20040E+02	.20040E+02	.72555E+00
42	.75050E+00	.20040E+02	.20040E+02	.77545E+00
43	.80040E+00	.20040E+02	.20040E+02	.82535E+00
44	.85030E+00	.20040E+02	.20040E+02	.87525E+00
45	.90020E+00	.20040E+02	.20040E+02	.92515E+00
46	.95010E+00	.20040E+02	.20040E+02	.97505E+00
47	.10000E+01	.20040E+02	.20040E+02	.10250E+01
48	.10499E+01	.20040E+02	.20040E+02	.10749E+01
49	.10998E+01	.20040E+02	.19472E+02	.11255E+01
50	.11512E+01	.18911E+02	.18359E+02	.11784E+01
51	.12056E+01	.17815E+02	.17279E+02	.12346E+01
52	.12635E+01	.16752E+02	.16232E+02	.12943E+01
53	.13252E+01	.15721E+02	.15218E+02	.13580E+01
54	.13909E+01	.14723E+02	.14237E+02	.14260E+01
55	.14611E+01	.13758E+02	.13288E+02	.14988E+01
56	.15364E+01	.12826E+02	.12372E+02	.15768E+01
57	.16173E+01	.11926E+02	.11488E+02	.16608E+01
58	.17044E+01	.11059E+02	.10638E+02	.17514E+01
59	.17984E+01	.10225E+02	.98196E+01	.18493E+01
60	.19003E+01	.94229E+01	.90344E+01	.19556E+01
61	.20110E+01	.86540E+01	.82819E+01	.20714E+01
62	.21318E+01	.79179E+01	.75621E+01	.21979E+01
63	.22641E+01	.72144E+01	.68750E+01	.23369E+01
64	.24097E+01	.65437E+01	.62206E+01	.24901E+01
65	.25705E+01	.59057E+01	.55990E+01	.26598E+01
66	.27493E+01	.53004E+01	.50100E+01	.28491E+01
67	.29490E+01	.47278E+01	.44538E+01	.30613E+01
68	.31738E+01	.41880E+01	.39303E+01	.33010E+01
69	.34285E+01	.36808E+01	.34395E+01	.35738E+01
70	.37196E+01	.32064E+01	.29815E+01	.38873E+01
71	.40554E+01	.27647E+01	.25561E+01	.42510E+01
72	.44473E+01	.23557E+01	.21635E+01	.46784E+01
73	.49103E+01	.19795E+01	.18036E+01	.51876E+01

K	Y(K)	G1(K)	G2(K)
1	0.	.19616E+02	.18967E+02
2	.52738E-01	.18330E+02	.17703E+02
3	.10924E+00	.17087E+02	.16482E+02
4	.16993E+00	.15889E+02	.15306E+02
5	.23529E+00	.14733E+02	.14172E+02
6	.30588E+00	.13622E+02	.13082E+02
7	.38235E+00	.12554E+02	.12036E+02
8	.46547E+00	.11530E+02	.11034E+02
9	.55615E+00	.10549E+02	.10075E+02
10	.65546E+00	.96116E+01	.91594E+01
11	.76470E+00	.87180E+01	.82876E+01
12	.88544E+00	.78680E+01	.74594E+01
13	.10196E+01	.70616E+01	.66747E+01
14	.11695E+01	.62988E+01	.59337E+01
15	.13382E+01	.55795E+01	.52363E+01
16	.15294E+01	.49039E+01	.45824E+01
17	.17479E+01	.42718E+01	.39721E+01
18	.20000E+01	.36834E+01	.34055E+01
19	.22941E+01	.31385E+01	.28824E+01
20	.26417E+01	.26372E+01	.24029E+01
21	.30588E+01	.21795E+01	.19670E+01
22	.35686E+01	.17654E+01	.15747E+01

AIRFOIL CP INTERPOLATED AT MESH MIDPOINTS

-.62005	-.93310	-.99886	-.91552	-.78805	-.65884	-.57667	-.52058	-.46253	-.40533
-.34669	-.29024	-.24981	-.20338	-.15500	-.10357	-.04889	.01203	.08102	.18388
.13984	-.22510	-.35281	-.38578	-.38582	-.36527	-.34118	-.31871	-.28447	-.25318
-.22485	-.18997	-.16652	-.13684	-.10243	-.06243	-.02272	.00925	.06270	.20789

I	JMX	KMX	ISUP	NS	DPHIMX	TTE
10	51	-1	0	0	.30275E-01	0.
20	54	-1	0	0	.37793E-02	0.
30	47	2	0	1	-.31927E-02	-.37203E-01
40	25	1	0	0	-.88577E-03	-.21847E-01
50	27	-1	0	0	-.57920E-03	.33738E-02
60	27	1	0	0	-.22779E-03	.29849E-02
70	20	-3	0	0	-.12368E-03	.41995E-02
80	22	-5	0	0	-.57585E-04	.41379E-02
90	17	-5	0	0	-.24974E-04	.39589E-02
100	18	-5	0	0	-.11480E-04	.38857E-02
110	71	17	0	0	.16741E-04	.38654E-02
120	55	-5	0	0	-.43619E-05	.38502E-02
130	46	-9	0	0	-.22216E-05	.38511E-02
140	36	-11	0	0	-.11129E-05	.38528E-02
142	34	-11	0	0	-.96593E-06	.38520E-02

RESULTS IN TUNNEL FLOW

CPSTAR = -.83370E+00

X(J-.5)	YMOD	CP(REF)	U	J	X(J)	V	DELTA PHI	DELTA V
-.02295	0.00000	.89501	-.53092	27	.00200	.79599		
	0.00000	.80344	-.47578			-.48157	-.00275	1.27756
.02695	.03972	-.62026	.46060	28	.05190	.25477		
	-.02403	.13740	-.00508			-.27912	.02049	.53389
.07685	.05243	-.93314	.46314	29	.10180	.14388		
	-.03796	-.22524	.13880			-.18164	.03667	.32552
.12675	.05961	-.99894	.47338	30	.15170	.07316		
	-.04702	-.35289	.18311			-.11979	.05115	.19295
.17665	.06326	-.91519	.42854	31	.20160	.02642		
	-.05300	-.38578	.19102			-.07831	.06301	.10472
.22655	.06458	-.78800	.36919	32	.25150	-.01312		
	-.05691	-.38581	.18755			-.04682	.07207	.03370
.27645	.06393	-.65896	.31101	33	.30140	-.03554		
	-.05924	-.36526	.17640			-.02388	.07879	-.01166
.32635	.06215	-.57676	.27436	34	.35130	-.05135		
	-.06044	-.34117	.16455			-.00578	.08427	-.04557
.37625	.05959	-.52065	.24968	35	.40120	-.06733		
	-.06072	-.31871	.15390			.01172	.08905	-.07905
.42615	.05623	-.46261	.22416	36	.45110	-.08126		
	-.06014	-.28448	.13798			.02424	.09335	-.10550
.47605	.05218	-.40540	.19889	37	.50100	-.09354		
	-.05893	-.25319	.12349			.03458	.09711	-.12812
.52595	.04751	-.34675	.17265	38	.55090	-.10304		
	-.05720	-.22486	.11043			.04508	.10021	-.14812
.57585	.04237	-.29027	.14687	39	.60080	-.10820		
	-.05495	-.18998	.09414			.05094	.10284	-.15914
.62575	.03697	-.24983	.12846	40	.65070	-.11632		
	-.05241	-.16652	.08327			.05960	.10510	-.17592
.67565	.03116	-.20340	.10718	41	.70060	-.12347		
	-.04944	-.13684	.06945			.06777	.10698	-.19123
.72555	.02500	-.15501	.08467	42	.75050	-.12992		
	-.04606	-.10243	.05325			.07516	.10855	-.20507
.77545	.01852	-.10358	.06032	43	.80040	-.13523		
	-.04231	-.06243	.03406			.07987	.10986	-.21509
.82535	.01177	-.04890	.03392	44	.85030	-.13955		
	-.03832	-.02272	.01463			.08200	.11082	-.22155
.87525	.00481	.01203	.00376	45	.90020	-.14169		
	-.03423	.00925	-.00091			.09101	.11106	-.23271
.92515	-.00226	.08101	-.03117	46	.95010	-.14482		
	-.02969	.06269	-.02655			.11387	.11083	-.25869
.97505	-.00949	.18384	-.08589	47	1.00000	-.13079		
	-.02400	.20786	-.10300			.08092	.11168	-.21171
1.02495	-.01601							
	-.01997							

OUTER BOUNDARY VELOCITIES

		X =	-.36772E+01	-.39083E+01	.42510E+01	.44473E+01
YU	YV		U	V	U	V
0.	.26361E-01		-.16305E-02	-.11308E-02	.12835E-01	-.48250E-03
.52738E-01	.80982E-01		-.15758E-02	-.11107E-02	.12969E-01	-.50906E-03
.10924E+00	.13958E+00		-.15158E-02	-.10874E-02	.13117E-01	-.53701E-03
.16993E+00	.20260E+00		-.14497E-02	-.10605E-02	.13279E-01	-.56645E-03
.23529E+00	.27057E+00		-.13770E-02	-.10293E-02	.13458E-01	-.59747E-03
.30588E+00	.34410E+00		-.12971E-02	-.99338E-03	.13658E-01	-.63018E-03
.38235E+00	.42389E+00		-.12092E-02	-.95196E-03	.13880E-01	-.66469E-03
.46547E+00	.51079E+00		-.11124E-02	-.90430E-03	.14129E-01	-.70110E-03
.55615E+00	.60577E+00		-.10061E-02	-.84951E-03	.14409E-01	-.73948E-03
.65546E+00	.71005E+00		-.88930E-03	-.78666E-03	.14726E-01	-.77994E-03
.76470E+00	.82503E+00		-.76117E-03	-.71472E-03	.15088E-01	-.82250E-03
.88544E+00	.95247E+00		-.62087E-03	-.63269E-03	.15502E-01	-.86715E-03
.10196E+01	.10945E+01		-.46761E-03	-.53964E-03	.15981E-01	-.91381E-03
.11695E+01	.12538E+01		-.30067E-03	-.43502E-03	.16537E-01	-.96224E-03
.13382E+01	.14337E+01		-.11935E-03	-.31900E-03	.17191E-01	-.10120E-02
.15294E+01	.16385E+01		.77354E-04	-.19335E-03	.17964E-01	-.10622E-02
.17479E+01	.18738E+01		.29184E-03	-.62918E-04	.18888E-01	-.11114E-02
0.	-.26361E-01		-.16305E-02	-.11486E-02	.12835E-01	-.45641E-03
-.52738E-01	-.80982E-01		-.16837E-02	-.11654E-02	.12704E-01	-.42892E-03
-.10924E+00	-.13958E+00		-.17387E-02	-.11813E-02	.12566E-01	-.39888E-03
-.16993E+00	-.20260E+00		-.17954E-02	-.11960E-02	.12423E-01	-.36594E-03
-.23529E+00	-.27057E+00		-.18533E-02	-.12089E-02	.12273E-01	-.32969E-03
-.30588E+00	-.34410E+00		-.19117E-02	-.12191E-02	.12117E-01	-.28963E-03
-.38235E+00	-.42389E+00		-.19696E-02	-.12256E-02	.11954E-01	-.24515E-03
-.46547E+00	-.51079E+00		-.20254E-02	-.12270E-02	.11784E-01	-.19553E-03
-.55615E+00	-.60577E+00		-.20768E-02	-.12213E-02	.11607E-01	-.13987E-03
-.65546E+00	-.71005E+00		-.21203E-02	-.12059E-02	.11422E-01	-.77076E-04
-.76470E+00	-.82503E+00		-.21508E-02	-.11772E-02	.11231E-01	-.57597E-05
-.88544E+00	-.95247E+00		-.21606E-02	-.11300E-02	.11033E-01	.75815E-04
-.10196E+01	-.10945E+01		-.21380E-02	-.10572E-02	.10827E-01	.16987E-03
-.11695E+01	-.12538E+01		-.20656E-02	-.94828E-03	.10614E-01	.27930E-03
-.13382E+01	-.14337E+01		-.19173E-02	-.78823E-03	.10393E-01	.40791E-03
-.15294E+01	-.16385E+01		-.16553E-02	-.55447E-03	.10159E-01	.56080E-03
-.17479E+01	-.18738E+01		-.12310E-02	-.21269E-03	.99053E-02	.74496E-03

		Y = .20000E+01	.20000E+01	-.20000E+01	-.20000E+01
XU	XV	U	V	U	V
-.36772E+01	-.39063E+01	.53134E-03		-.60797E-03	
-.32497E+01	-.34453E+01	.12457E-03	.44279E-03	.97594E-03	-.10989E-02
-.28857E+01	-.30534E+01	-.15474E-04	.76216E-03	-.54070E-02	-.54853E-02
-.25722E+01	-.27176E+01	-.29542E-04	.11301E-02	-.75968E-02	-.35789E-02
-.22993E+01	-.24265E+01	-.36859E-03	.16616E-02	-.62385E-02	-.10919E-02
-.20595E+01	-.21718E+01	-.55058E-04	.16842E-02	-.49950E-02	-.86245E-03
-.18472E+01	-.19470E+01	-.65282E-03	.23335E-02	-.54967E-02	-.21811E-02
-.16580E+01	-.17473E+01	-.39982E-03	.18844E-02	-.78425E-02	-.37291E-02
-.14882E+01	-.15685E+01	.10077E-02	.11086E-02	-.10522E-01	-.40495E-02
-.13349E+01	-.14077E+01	.22841E-02	.11269E-02	-.11137E-01	-.24411E-02
-.11960E+01	-.12621E+01	.31613E-02	.13842E-02	-.99739E-02	-.84673E-03
-.10694E+01	-.11298E+01	.41378E-02	.12488E-02	-.92035E-02	-.96951E-03
-.95367E+00	-.10090E+01	.54996E-02	.77141E-03	-.98645E-02	-.21237E-02
-.84736E+00	-.89828E+00	.72424E-02	.18633E-03	-.11031E-01	-.25743E-02
-.74940E+00	-.79640E+00	.92966E-02	-.38988E-03	-.11677E-01	-.19290E-02
-.65884E+00	-.70236E+00	.11585E-01	-.89301E-03	-.11255E-01	-.52962E-03
-.57487E+00	-.61528E+00	.13903E-01	-.11719E-02	-.99357E-02	.84650E-03
-.49680E+00	-.53443E+00	.16045E-01	-.12015E-02	-.81007E-02	.18059E-02
-.42402E+00	-.45914E+00	.17883E-01	-.10626E-02	-.60205E-02	.23301E-02
-.35603E+00	-.38888E+00	.19348E-01	-.84520E-03	-.38846E-02	.24505E-02
-.29235E+00	-.32315E+00	.20493E-01	-.72034E-03	-.18641E-02	.21745E-02
-.23260E+00	-.26153E+00	.21442E-01	-.80734E-03	-.10896E-03	.15346E-02
-.17641E+00	-.20365E+00	.22288E-01	-.10944E-02	.12843E-02	.62081E-03
-.12349E+00	-.14917E+00	.23096E-01	-.15513E-02	.22586E-02	-.47834E-03
-.72850E-01	-.97800E-01	.23927E-01	-.21572E-02	.27893E-02	-.16763E-02
-.22950E-01	-.47900E-01	.24837E-01	-.28398E-02	.28520E-02	-.29518E-02
.26950E-01	.20000E-02	.25823E-01	-.35724E-02	.25041E-02	-.40725E-02
.76850E-01	.51900E-01	.26840E-01	-.42748E-02	.18679E-02	-.48969E-02
.12675E+00	.10180E+00	.27839E-01	-.49287E-02	.10666E-02	-.53895E-02
.17665E+00	.15170E+00	.28774E-01	-.55208E-02	.22331E-03	-.55344E-02
.22655E+00	.20160E+00	.29597E-01	-.60415E-02	-.53860E-03	-.53328E-02
.27645E+00	.25150E+00	.30263E-01	-.64858E-02	-.10958E-02	-.48040E-02
.32635E+00	.30140E+00	.30732E-01	-.68643E-02	-.13572E-02	-.40312E-02
.37625E+00	.35130E+00	.31002E-01	-.72254E-02	-.13619E-02	-.32493E-02
.42615E+00	.40120E+00	.31077E-01	-.75829E-02	-.11820E-02	-.25505E-02
.47605E+00	.45110E+00	.30963E-01	-.79375E-02	-.88949E-03	-.19684E-02
.52595E+00	.50100E+00	.30664E-01	-.82904E-02	-.55649E-03	-.15245E-02
.57585E+00	.55090E+00	.30186E-01	-.86433E-02	-.25489E-03	-.12297E-02
.62575E+00	.60080E+00	.29534E-01	-.90008E-02	-.55999E-04	-.10828E-02
.67565E+00	.65070E+00	.28738E-01	-.94023E-02	.63589E-05	-.10202E-02
.72555E+00	.70060E+00	.27869E-01	-.99074E-02	-.40760E-04	-.94078E-03
.77545E+00	.75050E+00	.27002E-01	-.10521E-01	-.16475E-03	-.82464E-03
.82535E+00	.80040E+00	.26211E-01	-.11237E-01	-.33303E-03	-.66453E-03
.87525E+00	.85030E+00	.25572E-01	-.12039E-01	-.51300E-03	-.45729E-03
.92515E+00	.90020E+00	.25159E-01	-.12902E-01	-.67206E-03	-.20362E-03
.97505E+00	.95010E+00	.25041E-01	-.13781E-01	-.77933E-03	.89513E-04
.10250E+01	.10000E+01	.25172E-01	-.14481E-01	-.82660E-03	.38231E-03
.10749E+01	.10499E+01	.25427E-01	-.14860E-01	-.82152E-03	.64437E-03
.11255E+01	.10998E+01	.25684E-01	-.14900E-01	-.77106E-03	.87076E-03
.11784E+01	.11512E+01	.25806E-01	-.14575E-01	-.67855E-03	.10594E-02
.12346E+01	.12056E+01	.25606E-01	-.13864E-01	-.54637E-03	.12106E-02
.12943E+01	.12635E+01	.24824E-01	-.12750E-01	-.37994E-03	.13152E-02
.13580E+01	.13252E+01	.23297E-01	-.11467E-01	-.18764E-03	.13662E-02
.14260E+01	.13909E+01	.21198E-01	-.10496E-01	.18737E-04	.13590E-02
.14988E+01	.14611E+01	.18852E-01	-.10067E-01	.22139E-03	.12902E-02
.15768E+01	.15364E+01	.16759E-01	-.10358E-01	.39399E-03	.11614E-02
.16608E+01	.16173E+01	.15622E-01	-.11434E-01	.50217E-03	.98570E-03
.17514E+01	.17044E+01	.15633E-01	-.12608E-01	.56256E-03	.83892E-03
.18493E+01	.17984E+01	.16280E-01	-.13080E-01	.66230E-03	.80447E-03
.19556E+01	.19003E+01	.16674E-01	-.12520E-01	.94022E-03	.92460E-03
.20714E+01	.20110E+01	.15948E-01	-.11161E-01	.15944E-02	.12017E-02
.21979E+01	.21318E+01	.14635E-01	-.10285E-01	.25991E-02	.13982E-02
.23369E+01	.22641E+01	.14058E-01	-.10496E-01	.35493E-02	.12302E-02
.24901E+01	.24097E+01	.15023E-01	-.11228E-01	.40046E-02	.78450E-03
.26598E+01	.25705E+01	.16742E-01	-.11195E-01	.45961E-02	.82690E-03
.28491E+01	.27493E+01	.18178E-01	-.10134E-01	.63711E-02	.14518E-02
.30613E+01	.29490E+01	.18846E-01	-.84705E-02	.79775E-02	.11610E-02
.33010E+01	.31738E+01	.18654E-01	-.66817E-02	.80820E-02	.15079E-03
.35738E+01	.34285E+01	.18438E-01	-.54349E-02	.91194E-02	.40202E-03
.38873E+01	.37196E+01	.19876E-01	-.49051E-02	.90820E-02	-.67194E-04
.42510E+01	.40554E+01	.19993E-01	-.28507E-02	.96141E-02	.39198E-03

PHI IN VICINITY OF AIRFOIL

J	PHI(J,3,2)	PHI(J,2,2)	PHI(J,1,2)	PHI(J,1,1)	PHI(J,2,1)	PHI(J,3,1)
25	-.50429E-01	-.52140E-01	-.51801E-01	-.51801E-01	-.47526E-01	-.41340E-01
26	-.56935E-01	-.61584E-01	-.64478E-01	-.64478E-01	-.55613E-01	-.45505E-01
27	-.63086E-01	-.72724E-01	-.88220E-01	-.90971E-01	-.64400E-01	-.47826E-01
28	-.65524E-01	-.75528E-01	-.88473E-01	-.67988E-01	-.54556E-01	-.41802E-01
29	-.64117E-01	-.72372E-01	-.81547E-01	-.44877E-01	-.37283E-01	-.29235E-01
30	-.60009E-01	-.66159E-01	-.72410E-01	-.21256E-01	-.17363E-01	-.13186E-01
31	-.54407E-01	-.58722E-01	-.62878E-01	.12849E-03	.14006E-02	.29163E-02
32	-.48146E-01	-.50958E-01	-.53519E-01	.18551E-01	.17959E-01	.17653E-01
33	-.41744E-01	-.43355E-01	-.44717E-01	.34070E-01	.32345E-01	.30835E-01
34	-.35480E-01	-.36104E-01	-.36506E-01	.47761E-01	.45184E-01	.42741E-01
35	-.29518E-01	-.29291E-01	-.28826E-01	.60220E-01	.56829E-01	.53557E-01
36	-.23992E-01	-.23072E-01	-.21941E-01	.71405E-01	.67303E-01	.63313E-01
37	-.18966E-01	-.17464E-01	-.15779E-01	.81330E-01	.76612E-01	.72012E-01
38	-.14474E-01	-.12465E-01	-.10269E-01	.89945E-01	.84747E-01	.79659E-01
39	-.10555E-01	-.81310E-02	-.55710E-02	.97274E-01	.91751E-01	.86284E-01
40	-.72124E-02	-.43927E-02	-.14159E-02	.10368E+00	.97776E-01	.91949E-01
41	-.44962E-02	-.13206E-02	.20499E-02	.10903E+00	.10278E+00	.96639E-01
42	-.24723E-02	.99520E-03	.47069E-02	.11326E+00	.10670E+00	.10032E+00
43	-.12069E-02	.24616E-02	.64064E-02	.11627E+00	.10948E+00	.10294E+00
44	-.75203E-03	.30349E-02	.71366E-02	.11796E+00	.11102E+00	.10444E+00
45	-.11747E-02	.26741E-02	.70912E-02	.11815E+00	.11120E+00	.10477E+00
46	-.26281E-02	.10167E-02	.57664E-02	.11659E+00	.10984E+00	.10388E+00
47	-.52134E-02	-.26296E-02	.62668E-03	.11231E+00	.10672E+00	.10182E+00
48	-.84363E-02	-.74551E-02	-.72759E-02	.10440E+00	.10214E+00	.98992E-01
49	-.11408E-01	-.11255E-01	-.11746E-01	.99933E-01	.98504E-01	.96324E-01

I	JMX	KMX	ISUP	NS	DPHIMX	DA	UFAC	EU
1	71	17	0	4	-.54458E-01	0.	.10000E+01	.10000E+01
2	71	18	0	4	-.30782E-01	0.	.10000E+01	.10000E+01
3	71	17	0	4	-.19130E-01	0.	.10000E+01	.10000E+01
4	68	3	0	4	-.13160E-01	0.	.10000E+01	.10000E+01
5	68	2	0	4	-.96538E-02	0.	.10000E+01	.10000E+01
6	67	7	0	4	-.76971E-02	0.	.10000E+01	.10000E+01
7	66	7	0	4	-.63959E-02	0.	.10000E+01	.10000E+01
8	65	5	0	4	-.52869E-02	0.	.10000E+01	.10000E+01
9	64	2	0	4	-.44468E-02	0.	.10000E+01	.10000E+01
10	63	2	0	4	-.37217E-02	0.	.10000E+01	.10000E+01
11	62	2	0	4	-.31015E-02	0.	.10000E+01	.10000E+01
12	61	2	0	4	-.25836E-02	0.	.10000E+01	.10000E+01
13	60	2	0	4	-.21578E-02	0.	.10000E+01	.10000E+01
14	59	2	0	4	-.18095E-02	0.	.10000E+01	.10000E+01
15	59	-6	0	5	-.15884E-02	0.	.10000E+01	.10000E+01
16	58	-6	0	4	-.14043E-02	0.	.10000E+01	.10000E+01
17	57	-6	0	5	-.12393E-02	0.	.10000E+01	.10000E+01
18	56	-6	0	4	-.10929E-02	0.	.10000E+01	.10000E+01
19	55	-6	0	5	-.96379E-03	0.	.10000E+01	.10000E+01
20	54	4	0	5	-.85178E-03	-.38431E-03	.10000E+01	.10000E+01
21	53	6	0	5	-.75623E-03	-.74701E-03	.10000E+01	.10000E+01
22	52	6	0	4	-.67273E-03	-.10710E-02	.10000E+01	.10000E+01
23	51	6	0	4	-.60236E-03	-.13531E-02	.10000E+01	.10000E+01
24	50	6	0	4	-.54614E-03	-.15931E-02	.10000E+01	.10000E+01
25	49	6	0	4	-.50069E-03	-.17933E-02	.10000E+01	.10000E+01
26	48	6	0	4	-.46169E-03	-.19570E-02	.10000E+01	.10000E+01
27	48	8	0	4	-.42773E-03	-.20877E-02	.10000E+01	.10000E+01
28	47	8	0	4	-.40090E-03	-.21895E-02	.10000E+01	.10000E+01
29	46	8	0	4	-.37457E-03	-.22666E-02	.10000E+01	.10000E+01
30	45	8	0	4	-.34935E-03	-.23230E-02	.10000E+01	.10000E+01
31	44	8	0	4	-.32483E-03	-.23624E-02	.10000E+01	.10000E+01
32	43	8	0	4	-.30068E-03	-.23878E-02	.10000E+01	.10000E+01
33	42	8	0	4	-.27756E-03	-.24024E-02	.10000E+01	.10000E+01
34	43	1	0	4	-.25624E-03	-.24088E-02	.10000E+01	.10000E+01
35	42	1	0	4	-.23976E-03	-.24092E-02	.10000E+01	.10000E+01
36	41	1	0	4	-.22366E-03	-.24054E-02	.10000E+01	.10000E+01
37	40	1	0	4	-.20834E-03	-.23990E-02	.10000E+01	.10000E+01
38	39	1	0	4	-.19403E-03	-.23909E-02	.10000E+01	.10000E+01
39	38	1	0	4	-.18090E-03	-.23821E-02	.10000E+01	.10000E+01
40	38	1	0	4	-.16990E-03	-.23731E-02	.10000E+01	.10000E+01
41	37	1	0	4	-.15988E-03	-.23644E-02	.10000E+01	.10000E+01
42	36	1	0	4	-.15090E-03	-.23562E-02	.10000E+01	.10000E+01
43	35	1	0	4	-.14241E-03	-.23487E-02	.10000E+01	.10000E+01
44	34	1	0	4	-.13307E-03	-.23420E-02	.10000E+01	.10000E+01
45	32	1	0	4	-.12390E-03	-.23363E-02	.10000E+01	.10000E+01
46	32	1	0	4	-.10928E-03	-.23316E-02	.10000E+01	.10000E+01
47	43	-1	0	4	-.97027E-04	-.23282E-02	.10000E+01	.10000E+01
48	48	-1	0	3	-.17427E-03	-.22935E-02	.99890E+00	.55662E-01
49	47	-1	0	3	-.12114E-03	-.22616E-02	.99890E+00	.55662E-01
50	48	-1	0	3	-.14912E-03	-.22527E-02	.99890E+00	.55662E-01
51	45	-2	0	3	-.10182E-03	-.22417E-02	.99890E+00	.55662E-01
52	48	-1	0	3	-.12091E-03	-.22425E-02	.99890E+00	.55662E-01
53	43	-2	0	3	-.89928E-04	-.22400E-02	.99890E+00	.55662E-01
54	48	-1	0	3	-.20101E-03	-.22087E-02	.99769E+00	.55611E-01
55	47	-1	0	3	-.11749E-03	-.21766E-02	.99769E+00	.55611E-01
56	48	-1	0	3	-.16395E-03	-.21727E-02	.99769E+00	.55611E-01
57	45	-2	0	3	-.94975E-04	-.21636E-02	.99769E+00	.55611E-01
58	48	-1	0	3	-.12745E-03	-.21690E-02	.99769E+00	.55611E-01
59	43	-2	0	3	-.82327E-04	-.21687E-02	.99769E+00	.55611E-01
60	50	1	0	3	-.76175E-04	-.21949E-02	.99830E+00	.56199E-01
61	41	-2	0	3	-.68234E-04	-.22157E-02	.99830E+00	.56199E-01
62	40	-2	0	3	-.64215E-04	-.22293E-02	.99830E+00	.56199E-01
63	48	-1	0	3	-.63532E-04	-.22412E-02	.99830E+00	.56199E-01
64	38	-2	0	3	-.59048E-04	-.22498E-02	.99830E+00	.56199E-01

STEPS 65 - 195 OMITTED

196	49	-1	0	4	-.20458E-04	-.25551E-02	.10014E+01	.54774E-01
197	50	-1	0	4	.14432E-04	-.25520E-02	.10014E+01	.54774E-01
198	50	-1	0	4	-.13545E-04	-.25506E-02	.10014E+01	.54774E-01
199	20	4	0	4	-.96440E-05	-.25476E-02	.10014E+01	.54774E-01
200	48	-1	0	4	.72986E-04	-.25744E-02	.10024E+01	.54666E-01
201	48	-1	0	4	-.66188E-04	-.25988E-02	.10024E+01	.54666E-01
202	48	-1	0	4	.58745E-04	-.26049E-02	.10024E+01	.54666E-01
203	48	-1	0	4	-.48508E-04	-.26130E-02	.10024E+01	.54666E-01
204	48	-1	0	4	.40135E-04	-.26122E-02	.10024E+01	.54666E-01
205	48	-1	0	4	-.32088E-04	-.26144E-02	.10024E+01	.54666E-01
206	49	-1	0	4	.25919E-04	-.26113E-02	.10024E+01	.54666E-01
207	49	-1	0	4	-.20915E-04	-.26107E-02	.10024E+01	.54666E-01
208	50	-1	0	4	.16437E-04	-.26071E-02	.10024E+01	.54666E-01
209	50	-1	0	4	-.13617E-04	-.26053E-02	.10024E+01	.54666E-01
210	51	-1	0	4	.10321E-04	-.26018E-02	.10024E+01	.54666E-01
211	19	4	0	4	-.91039E-05	-.25996E-02	.10024E+01	.54666E-01
212	48	-1	0	4	-.34696E-04	-.25823E-02	.10019E+01	.54700E-01
213	48	-1	0	4	.29855E-04	-.25668E-02	.10019E+01	.54700E-01
214	48	-1	0	4	-.28617E-04	-.25603E-02	.10019E+01	.54700E-01
215	48	-1	0	4	.21697E-04	-.25533E-02	.10019E+01	.54700E-01
216	48	-1	0	4	-.20077E-04	-.25510E-02	.10019E+01	.54700E-01
217	48	-1	0	4	.13892E-04	-.25475E-02	.10019E+01	.54700E-01
218	49	-1	0	4	-.13530E-04	-.25469E-02	.10019E+01	.54700E-01
219	49	-1	0	4	.85148E-05	-.25453E-02	.10019E+01	.54700E-01
220	29	2	0	4	-.16609E-04	-.25526E-02	.10021E+01	.54752E-01
221	48	-1	0	4	-.13042E-04	-.25588E-02	.10021E+01	.54752E-01
222	48	-1	0	4	.10227E-04	-.25612E-02	.10021E+01	.54752E-01
223	48	-1	0	4	-.10210E-04	-.25638E-02	.10021E+01	.54752E-01
224	48	-1	0	4	.69035E-05	-.25646E-02	.10021E+01	.54752E-01
225	29	2	0	4	-.20183E-04	-.25736E-02	.10024E+01	.54731E-01
226	48	-1	0	4	-.15409E-04	-.25810E-02	.10024E+01	.54731E-01
227	48	-1	0	4	.13132E-04	-.25836E-02	.10024E+01	.54731E-01
228	48	-1	0	4	-.11849E-04	-.25862E-02	.10024E+01	.54731E-01
229	48	-1	0	4	.90289E-05	-.25864E-02	.10024E+01	.54731E-01
230	29	2	0	4	-.22689E-04	-.25957E-02	.10027E+01	.54729E-01
231	48	-1	0	4	-.15839E-04	-.26031E-02	.10027E+01	.54729E-01
232	48	-1	0	4	.14335E-04	-.26053E-02	.10027E+01	.54729E-01
233	48	-1	0	4	-.12196E-04	-.26074E-02	.10027E+01	.54729E-01
234	48	-1	0	4	.10012E-04	-.26070E-02	.10027E+01	.54729E-01
235	48	-1	0	4	-.82390E-05	-.26072E-02	.10027E+01	.54729E-01
236	50	-2	0	4	-.71206E-05	-.26016E-02	.10025E+01	.54758E-01
237	22	2	0	4	-.57290E-05	-.25969E-02	.10025E+01	.54758E-01
238	48	-1	0	4	-.59965E-05	-.25942E-02	.10025E+01	.54758E-01
239	20	2	0	4	-.46322E-05	-.25917E-02	.10025E+01	.54758E-01
240	48	-1	0	4	-.44780E-05	-.25901E-02	.10025E+01	.54758E-01
241	48	-1	0	4	.89621E-05	-.25907E-02	.10026E+01	.54781E-01
242	48	-1	0	4	-.83757E-05	-.25918E-02	.10026E+01	.54781E-01
243	48	-1	0	4	.64344E-05	-.25914E-02	.10026E+01	.54781E-01
244	48	-1	0	4	-.58743E-05	-.25915E-02	.10026E+01	.54781E-01
245	48	-1	0	4	.41093E-05	-.25910E-02	.10026E+01	.54781E-01
246	48	-1	0	4	-.70167E-05	-.25898E-02	.10026E+01	.54792E-01
247	48	-1	0	4	.51502E-05	-.25882E-02	.10026E+01	.54792E-01
248	48	-1	0	4	-.50911E-05	-.25878E-02	.10026E+01	.54792E-01
249	48	-1	0	4	.33549E-05	-.25869E-02	.10026E+01	.54792E-01
250	48	-1	0	4	-.35104E-05	-.25867E-02	.10026E+01	.54792E-01
251	48	-1	0	4	.35741E-05	-.25867E-02	.10026E+01	.54797E-01
252	48	-1	0	4	-.37409E-05	-.25870E-02	.10026E+01	.54797E-01
253	48	-1	0	4	.23641E-05	-.25868E-02	.10026E+01	.54797E-01
254	48	-1	0	4	-.26409E-05	-.25869E-02	.10026E+01	.54797E-01
255	48	-1	0	4	.14119E-05	-.25867E-02	.10026E+01	.54797E-01
256	48	-1	0	4	-.26132E-05	-.25864E-02	.10026E+01	.54799E-01
257	48	-1	0	4	.14239E-05	-.25860E-02	.10026E+01	.54799E-01
258	49	-1	0	4	-.19326E-05	-.25859E-02	.10026E+01	.54799E-01
259	21	7	0	4	-.93532E-06	-.25856E-02	.10026E+01	.54799E-01
260	49	-1	0	4	-.14109E-05	-.25855E-02	.10026E+01	.54799E-01

EQUIVALENT FREE AIR (U AND V ARE PERTURBATIONS FROM UINF BUT NORMALIZED BY UREF)

AMINF = .68906, UINF/UREF = 1.00258, CPSTAR = -.82530E+00, QFAC = 1.00393 ALPHA CORRECTION = -.25855E-02

X(J-.5)	YMOD	CP(INF)	U	J	X(J)	V	DELTA PHI	DELTA V
-.02295	0.00000	.89500	-.53133	27	.00200	.79856		
	0.00000	.80900	-.48184			-.47898	-.00247	1.27754
.02695	.03975	-.61591	.46041	28	.05190	.25735		
	-.02384	.14563	-.01086			-.27652	.02105	.53387
.07685	.05255	-.92393	.46095	29	.10180	.14646		
	-.03760	-.21455	.13314			-.17905	.03740	.32551
.12675	.05984	-.98364	.46830	30	.15170	.07574		
	-.04651	-.34113	.17753			-.11720	.05191	.19294
.17665	.06361	-.89566	.42122	31	.20160	.02900		
	-.05235	-.37360	.18552			-.07571	.06367	.10471
.22655	.06506	-.76973	.36207	32	.25150	-.01054		
	-.05612	-.37343	.18209			-.04423	.07266	.03369
.27645	.06453	-.64438	.30522	33	.30140	-.03296		
	-.05832	-.35285	.17098			-.02128	.07935	-.01167
.32635	.06289	-.56172	.26813	34	.35130	-.04877		
	-.05938	-.32874	.15913			-.00319	.08479	-.04558
.37625	.06047	-.50541	.24318	35	.40120	-.06475		
	-.05953	-.30620	.14845			.01431	.08952	-.07907
.42615	.05724	-.44742	.21751	36	.45110	-.07868		
	-.05882	-.27201	.13251			.02683	.09376	-.10551
.47605	.05333	-.39036	.19214	37	.50100	-.09096		
	-.05749	-.24073	.11799			.03718	.09746	-.12814
.52595	.04880	-.33194	.16583	38	.55090	-.10046		
	-.05564	-.21236	.10486			.04768	.10050	-.14814
.57585	.04380	-.27570	.14001	39	.60080	-.10562		
	-.05326	-.17752	.08853			.05354	.10307	-.15915
.62575	.03854	-.23531	.12150	40	.65070	-.11374		
	-.05060	-.15397	.07757			.06220	.10527	-.17593
.67565	.03288	-.18908	.10018	41	.70060	-.12089		
	-.04750	-.12426	.06367			.07036	.10709	-.19125
.72555	.02686	-.14094	.07764	42	.75050	-.12734		
	-.04400	-.08984	.04739			.07775	.10860	-.20509
.77545	.02053	-.08983	.05330	43	.80040	-.13265		
	-.04013	-.04989	.02813			.08246	.10985	-.21510
.82535	.01392	-.03554	.02691	44	.85030	-.13697		
	-.03603	-.01023	.00861			.08459	.11077	-.22156
.87525	.00711	.02491	-.00319	45	.90020	-.13911		
	-.03182	.02181	-.00705			.09361	.11096	-.23272
.92515	.00018	.09331	-.03803	46	.95010	-.14224		
	-.02716	.07518	-.03280			.11646	.11070	-.25870
.97505	-.00690	.19517	-.09254	47	1.00000	-.12821		
	-.02136	.21924	-.10918			.08352	.11153	-.21173
1.02495	-.01328							
	-.01720							

EXPERIMENTAL CP BASED ON CORRECTED AMINF, CL = .22248

X	CP(INF)
.02695	-.61248
	.14442
.07685	-.92430
	-.21909
.12675	-.98981
	-.34629
.17665	-.90680
	-.37913
.22655	-.77983
	-.37918
.27645	-.65113
	-.35871
.32635	-.56927
	-.33471
.37625	-.51340
	-.31232
.42615	-.45559
	-.27822
.47605	-.39861
	-.24706
.52595	-.34020
	-.21884
.57585	-.28396
	-.18409
.62575	-.24370
	-.16073
.67565	-.19745
	-.13117
.72555	-.14925
	-.09689
.77545	-.09803
	-.05705
.82535	-.04357
	-.01750
.87525	.01712
	.01435
.92515	.08584
	.06759
.97505	.18829
	.21221

RMS DELTA CP = .70930E-02

UPPER SURFACE		LOWER SURFACE	
X	CP(INF)	X	CP(INF)
.00022	1.08939	.00022	1.08939
.01436	-.32484	.01172	.50168
.02822	-.61813	.02434	.18546
.05297	-.83806	.04994	-.09600
.07798	-.92659	.07417	-.20924
.10296	-.98393	.09855	-.29178
.15231	-.95264	.14860	-.36580
.20155	-.85013	.19846	-.38267
.25228	-.70696	.24811	-.37188
.30200	-.60486	.29807	-.34786
.35197	-.53853	.34861	-.32497
.40145	-.48644	.39795	-.29966
.45146	-.42429	.44826	-.26199
.50149	-.37157	.49806	-.23617
.55082	-.30872	.54869	-.20280
.60089	-.26364	.59798	-.17166
.65075	-.22182	.64853	-.15034
.70067	-.17255	.69885	-.11356
.74982	-.12580	.74836	-.08144
.80091	-.06963	.79859	-.03607
.85039	-.01527	.84924	-.00326
.89945	.05028	.89914	.03500
.94878	.12668	.94766	.11670
.98750	.22079	.98750	.26259

I	JMX	KMX	ISUP	NS	DPHIMX	
10	65	-1	0	4	.73865E-04	
20	46	18	0	4	.16297E-04	
30	37	19	0	4	.70191E-05	
40	22	-3	0	4	-.40991E-05	
50	15	-3	0	4	-.17667E-05	
55	11	-4	0	4	-.84840E-06	0.

MODEL PERTURBATION (U AND V ARE PERTURBATIONS FROM UINF BUT NORMALIZED BY UREF)

X(J-.5)	YMOD	CP(INF)	U	J	X(J)	V	DELTA PHI	DELTA V
-.02295	0.00000	.89752	-.53394	27	.00200	.80010		
	0.00000	.80539	-.47880			-.47746	-.00275	1.27756
.02695	.03982	-.60690	.45661	28	.05190	.25864		
	-.02376	.14161	-.00907			-.27525	.02049	.53389
.07685	.05270	-.91793	.45853	29	.10180	.14775		
	-.03746	-.21731	.13419			-.17777	.03667	.32552
.12675	.06005	-.98236	.46790	30	.15170	.07673		
	-.04631	-.34173	.17763			-.11622	.05115	.19296
.17665	.06387	-.89860	.42262	31	.20160	.02964		
	-.05210	-.37290	.18510			-.07509	.06301	.10473
.22655	.06534	-.77237	.36328	32	.25150	-.01012		
	-.05583	-.37254	.18164			-.04383	.07207	.03371
.27645	.06484	-.64479	.30539	33	.30140	-.03244		
	-.05802	-.35247	.17079			-.02079	.07879	-.01165
.32635	.06323	-.56277	.26859	34	.35130	-.04829		
	-.05905	-.32801	.15878			-.00274	.08427	-.04556
.37625	.06082	-.50674	.24377	35	.40120	-.06434		
	-.05919	-.30521	.14799			.01470	.08905	-.07904
.42615	.05762	-.44889	.21816	36	.45110	-.07834		
	-.05845	-.27087	.13198			.02715	.09335	-.10549
.47605	.05372	-.39187	.19281	37	.50100	-.09068		
	-.05710	-.23951	.11741			.03743	.09711	-.12811
.52595	.04921	-.33341	.16650	38	.55090	-.10024		
	-.05524	-.21112	.10428			.04787	.10021	-.14811
.57585	.04422	-.27713	.14067	39	.60080	-.10546		
	-.05286	-.17628	.08794			.05367	.10284	-.15912
.62575	.03897	-.23672	.12216	40	.65070	-.11364		
	-.05019	-.15273	.07697			.06226	.10510	-.17590
.67565	.03331	-.19042	.10082	41	.70060	-.12085		
	-.04709	-.12305	.06309			.07037	.10698	-.19122
.72555	.02730	-.14219	.07826	42	.75050	-.12736		
	-.04359	-.08871	.04683			.07769	.10855	-.20505
.77545	.02096	-.09097	.05387	43	.80040	-.13274		
	-.03972	-.04885	.02760			.08233	.10986	-.21507
.82535	.01435	-.03653	.02743	44	.85030	-.13713		
	-.03562	-.00933	.00815			.08440	.11082	-.22153
.87525	.00753	.02414	-.00277	45	.90020	-.13932		
	-.03142	.02252	-.00744			.09337	.11106	-.23269
.92515	.00059	.09275	-.03771	46	.95010	-.14246		
	-.02677	.07568	-.03308			.11620	.11083	-.25867
.97505	-.00650	.19475	-.09228	47	1.00000	-.12854		
	-.02099	.21958	-.10939			.08315	.11168	-.21169
1.02495	-.01289							
	-.01685							

VELOCITIES ON CENTER LINE

XV	VF	VW	XU	UF	UW
-.39083E+01	.30985E-02	-.42382E-02			
-.34453E+01	.34901E-02	-.41572E-02	-.36772E+01	-.16325E-02	.20171E-05
-.30534E+01	.39067E-02	-.41839E-02	-.32497E+01	-.19479E-02	-.16033E-03
-.27176E+01	.43519E-02	-.42075E-02	-.28857E+01	-.23359E-02	-.34861E-03
-.24265E+01	.48288E-02	-.42212E-02	-.25722E+01	-.27996E-02	-.47758E-03
-.21718E+01	.53414E-02	-.42316E-02	-.22993E+01	-.33465E-02	-.52281E-03
-.19470E+01	.58940E-02	-.42379E-02	-.20595E+01	-.39878E-02	-.49086E-03
-.17473E+01	.64916E-02	-.42368E-02	-.18472E+01	-.47383E-02	-.39341E-03
-.15685E+01	.71402E-02	-.42262E-02	-.16580E+01	-.56168E-02	-.24121E-03
-.14077E+01	.78470E-02	-.42066E-02	-.14882E+01	-.66470E-02	-.44745E-04
-.12621E+01	.86206E-02	-.41796E-02	-.13349E+01	-.78589E-02	.18538E-03
-.11298E+01	.94715E-02	-.41472E-02	-.11960E+01	-.92900E-02	.43889E-03
-.10090E+01	.10412E-01	-.41111E-02	-.10694E+01	-.10988E-01	.70643E-03
-.89828E+00	.11459E-01	-.40730E-02	-.95367E+00	-.13016E-01	.97995E-03
-.79640E+00	.12632E-01	-.40341E-02	-.84736E+00	-.15453E-01	.12528E-02
-.70236E+00	.13958E-01	-.39955E-02	-.74940E+00	-.18409E-01	.15197E-02
-.61528E+00	.15469E-01	-.39577E-02	-.65884E+00	-.22030E-01	.17767E-02
-.53443E+00	.17211E-01	-.39215E-02	-.57487E+00	-.26521E-01	.20210E-02
-.45914E+00	.19246E-01	-.38872E-02	-.49680E+00	-.32178E-01	.22505E-02
-.38888E+00	.21661E-01	-.38555E-02	-.42402E+00	-.39442E-01	.24633E-02
-.32315E+00	.24584E-01	-.38269E-02	-.35603E+00	-.49000E-01	.26577E-02
-.26153E+00	.28207E-01	-.38023E-02	-.29235E+00	-.62000E-01	.28316E-02
-.20365E+00	.32838E-01	-.37832E-02	-.23260E+00	-.80532E-01	.29815E-02
-.14917E+00	.38985E-01	-.37719E-02	-.17641E+00	-.10894E+00	.31015E-02
-.97800E-01	.47528E-01	-.37731E-02	-.12349E+00	-.15790E+00	.31796E-02
-.47900E-01	.60424E-01	-.37968E-02	-.72850E-01	-.25723E+00	.31836E-02
.20000E-02	.80010E+00	-.41126E-02	-.22950E-01	-.53394E+00	.30208E-02
	-.47746E+00	-.41146E-02		-.47880E+00	.30208E-02
.51900E-01	.25864E+00	-.38705E-02	.26950E-01	.45661E+00	.39900E-02
	-.27525E+00	-.38701E-02		-.90651E-02	.39900E-02
.10180E+00	.14775E+00	-.38704E-02	.76850E-01	.45853E+00	.46107E-02
	-.17777E+00	-.38681E-02		.13419E+00	.46107E-02
.15170E+00	.76734E-01	-.35711E-02	.12675E+00	.46790E+00	.54810E-02
	-.11622E+00	-.35667E-02		.17763E+00	.54810E-02
.20160E+00	.29644E-01	-.32258E-02	.17665E+00	.42262E+00	.59203E-02
	-.75085E-01	-.32197E-02		.18510E+00	.59203E-02
.25150E+00	-.10120E-01	-.30021E-02	.22655E+00	.36328E+00	.59122E-02
	-.43830E-01	-.29942E-02		.18164E+00	.59122E-02
.30140E+00	-.32440E-01	-.30957E-02	.27645E+00	.30539E+00	.56159E-02
	-.20790E-01	-.30863E-02		.17079E+00	.56159E-02
.35130E+00	-.48292E-01	-.30545E-02	.32635E+00	.26859E+00	.57691E-02
	-.27356E-02	-.30437E-02		.15878E+00	.57691E-02
.40120E+00	-.64336E-01	-.29940E-02	.37625E+00	.24377E+00	.59114E-02
	.14703E-01	-.29818E-02		.14799E+00	.59114E-02
.45110E+00	-.78336E-01	-.29257E-02	.42615E+00	.21816E+00	.59967E-02
	.27149E-01	-.29122E-02		.13198E+00	.59967E-02

.50100E+00	-.90681E-01	-.28560E-02	.47605E+00	.19281E+00	.60766E-02
	.37425E-01	-.28413E-02		.11741E+00	.60766E-02
.55090E+00	-.10024E+00	-.27975E-02	.52595E+00	.16650E+00	.61487E-02
	.47866E-01	-.27819E-02		.10428E+00	.61487E-02
.60080E+00	-.10546E+00	-.27397E-02	.57585E+00	.14067E+00	.62023E-02
	.53667E-01	-.27231E-02		.87941E-01	.62023E-02
.65070E+00	-.11364E+00	-.26760E-02	.62575E+00	.12216E+00	.62973E-02
	.62263E-01	-.26587E-02		.76972E-01	.62973E-02
.70060E+00	-.12085E+00	-.26144E-02	.67565E+00	.10082E+00	.63644E-02
	.70366E-01	-.25964E-02		.63090E-01	.63644E-02
.75050E+00	-.12736E+00	-.25528E-02	.72555E+00	.78256E-01	.64180E-02
	.77691E-01	-.25343E-02		.46828E-01	.64180E-02
.80040E+00	-.13274E+00	-.24875E-02	.77545E+00	.53869E-01	.64560E-02
	.82334E-01	-.24685E-02		.27603E-01	.64560E-02
.85030E+00	-.13713E+00	-.24172E-02	.82535E+00	.27430E-01	.64880E-02
	.84395E-01	-.23978E-02		.81457E-02	.64880E-02
.90020E+00	-.13932E+00	-.23705E-02	.87525E+00	-.27686E-02	.65243E-02
	.93365E-01	-.23507E-02		-.74357E-02	.65243E-02
.95010E+00	-.14246E+00	-.23550E-02	.92515E+00	-.37708E-01	.65342E-02
	.11620E+00	-.23347E-02		-.33083E-01	.65342E-02
.10000E+01	-.12854E+00	-.22484E-02	.97505E+00	-.92281E-01	.63890E-02
	.83152E-01	-.22277E-02		-.10939E+00	.63890E-02
.10499E+01	-.17579E-01	-.22009E-02	.10250E+01	-.16463E+00	.62575E-02
.10998E+01	-.16074E-01	-.21420E-02	.10749E+01	-.96249E-01	.66665E-02
.11512E+01	-.14897E-01	-.20789E-02	.11255E+01	-.67937E-01	.69045E-02
.12056E+01	-.13887E-01	-.20103E-02	.11784E+01	-.52070E-01	.71082E-02
.12635E+01	-.12987E-01	-.19361E-02	.12346E+01	-.41608E-01	.73031E-02
.13252E+01	-.12170E-01	-.18563E-02	.12943E+01	-.34052E-01	.74975E-02
.13909E+01	-.11417E-01	-.17707E-02	.13580E+01	-.28300E-01	.76957E-02
.14611E+01	-.10718E-01	-.16791E-02	.14260E+01	-.23769E-01	.79009E-02
.15364E+01	-.10065E-01	-.15811E-02	.14988E+01	-.20116E-01	.81156E-02
.16173E+01	-.94510E-02	-.14765E-02	.15768E+01	-.17118E-01	.83424E-02
.17044E+01	-.88720E-02	-.13646E-02	.16608E+01	-.14624E-01	.85839E-02
.17984E+01	-.83240E-02	-.12449E-02	.17514E+01	-.12529E-01	.88430E-02
.19003E+01	-.78040E-02	-.11163E-02	.18493E+01	-.10752E-01	.91227E-02
.20110E+01	-.73093E-02	-.97776E-03	.19556E+01	-.92365E-02	.94265E-02
.21318E+01	-.68378E-02	-.82741E-03	.20714E+01	-.79357E-02	.97581E-02
.22641E+01	-.63875E-02	-.66278E-03	.21979E+01	-.68144E-02	.10121E-01
.24097E+01	-.59568E-02	-.48040E-03	.23369E+01	-.58444E-02	.10520E-01
.25705E+01	-.55442E-02	-.27548E-03	.24901E+01	-.50030E-02	.10956E-01
.27493E+01	-.51484E-02	-.41664E-04	.26598E+01	-.42719E-02	.11430E-01
.29490E+01	-.47682E-02	.22916E-03	.28491E+01	-.36361E-02	.11939E-01
.31738E+01	-.44027E-02	.54702E-03	.30613E+01	-.30836E-02	.12473E-01
.34285E+01	-.40509E-02	.92456E-03	.33010E+01	-.26050E-02	.13016E-01
.37196E+01	-.37119E-02	.13785E-02	.35738E+01	-.21935E-02	.13541E-01
.40554E+01	-.33851E-02	.19305E-02	.38873E+01	-.18450E-02	.14017E-01
.44473E+01	-.30697E-02	.26002E-02	.42510E+01	-.15592E-02	.14394E-01

	VW	UW	RESULTANT
MEAN OVER MODEL	-.29383E-02	.58156E-02	
STANDARD DEVIATION OVER MODEL	.52191E-03	.87955E-03	.10227E-02

REFERENCES

1. Kemp, William B., Jr.: Toward the Correctable-Interference Transonic Wind Tunnel. Proceedings - AIAA 9th Aerodynamic Testing Conference, June 1976, pp. 31-38.

2. Kemp, William B., Jr.: Transonic Assessment of Two-Dimensional Wind Tunnel Wall Interference Using Measured Wall Pressures. Advanced Airfoil Technology Research - Volume I, NASA CP-2045, Part 2, 1979, pp. 473-486.

3. Kemp, William B., Jr.: TWINTAN: A Program for Transonic Wall Interference Assessment in Two-Dimensional Wind Tunnels. NASA TM-81819, 1980.

4. Barnwell, Richard W.: Similarity Rule for Sidewall Boundary-Layer Effect in Two-Dimensional Wind Tunnels. AIAA Journal, Vol. 18, No. 9, Sept. 1980, pp 1149-1151.

5. Sewall, W. G.: The Effects of the Sidewall Boundary Layers on Two-Dimensional Subsonic and Transonic Wind Tunnels. AIAA Journal, Vol. 20, no. 9, Sept. 1982, pp. 1253-1256.

6. Kemp, William B., Jr.; and Adcock, J. B.: Combined Four-Wall Interference Assessment in Two-Dimensional Airfoil Tests. AIAA Paper No. 82-0586, March 1982.

7. Murman, E. M.: A Correction Method for Transonic Wind-Tunnel Wall Interference. AIAA Paper 79-1533, July 1979.

8. Klunker, E. B.: Contribution to Methods for Calculating the Flow About Thin Lifting Wings at Transonic Speeds - Analytic Expressions for the Far Field. NASA TN D-6530, 1971.

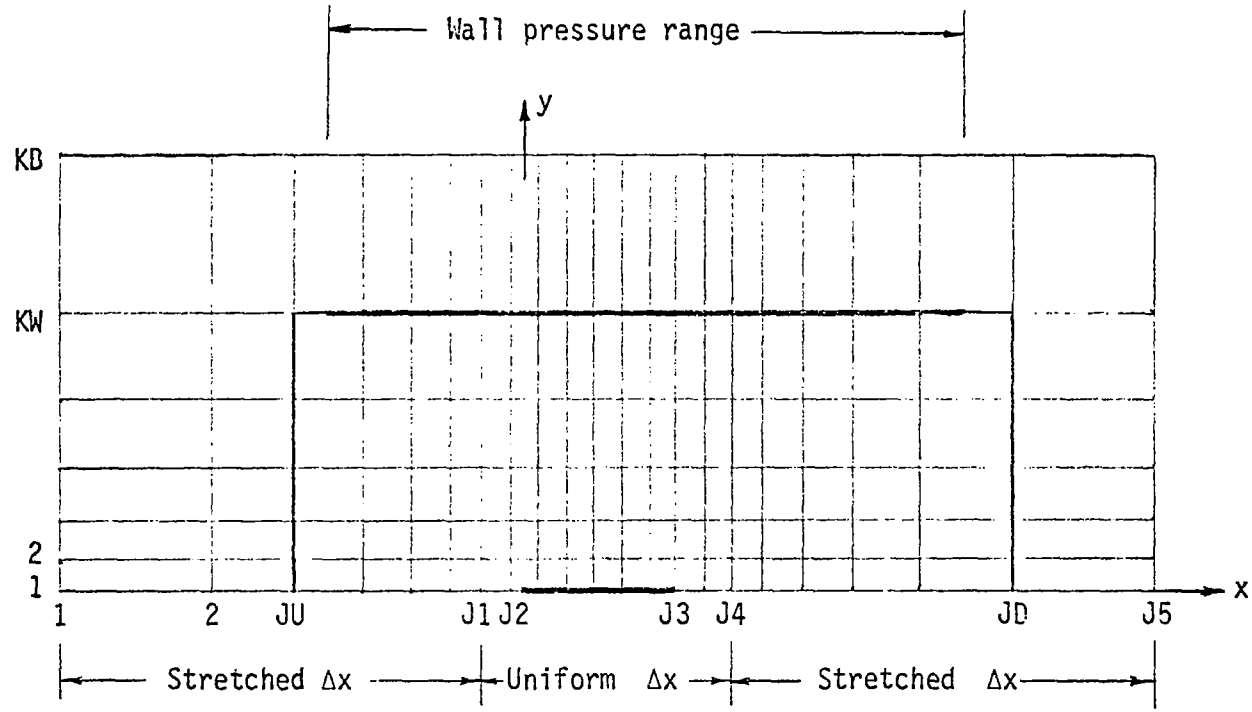

Figure 1.- Schematic representation of upper half of computational grid. Lower half is mirror image about x axis.

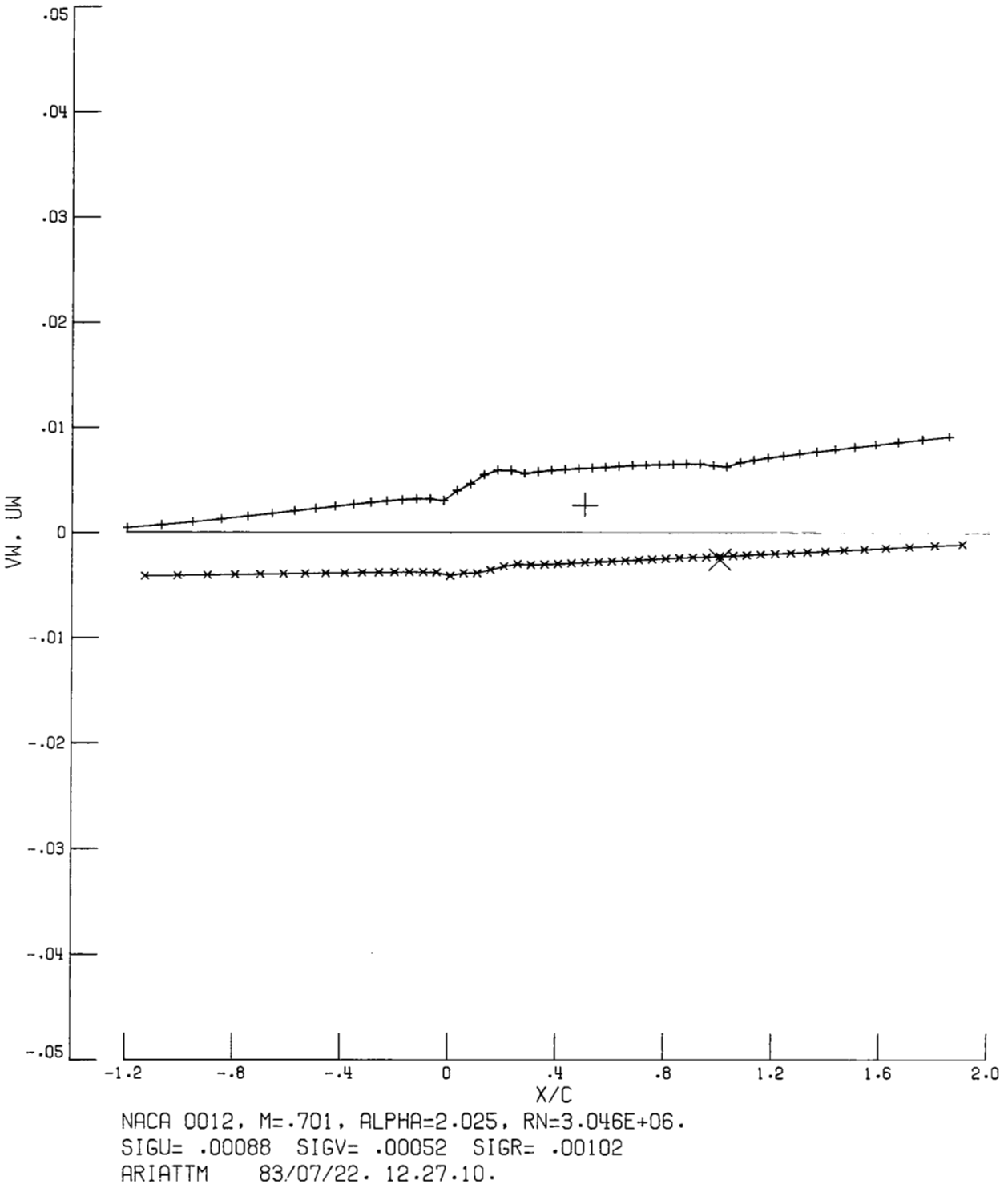

Figure 2.- First frame of plotted output for sample case.

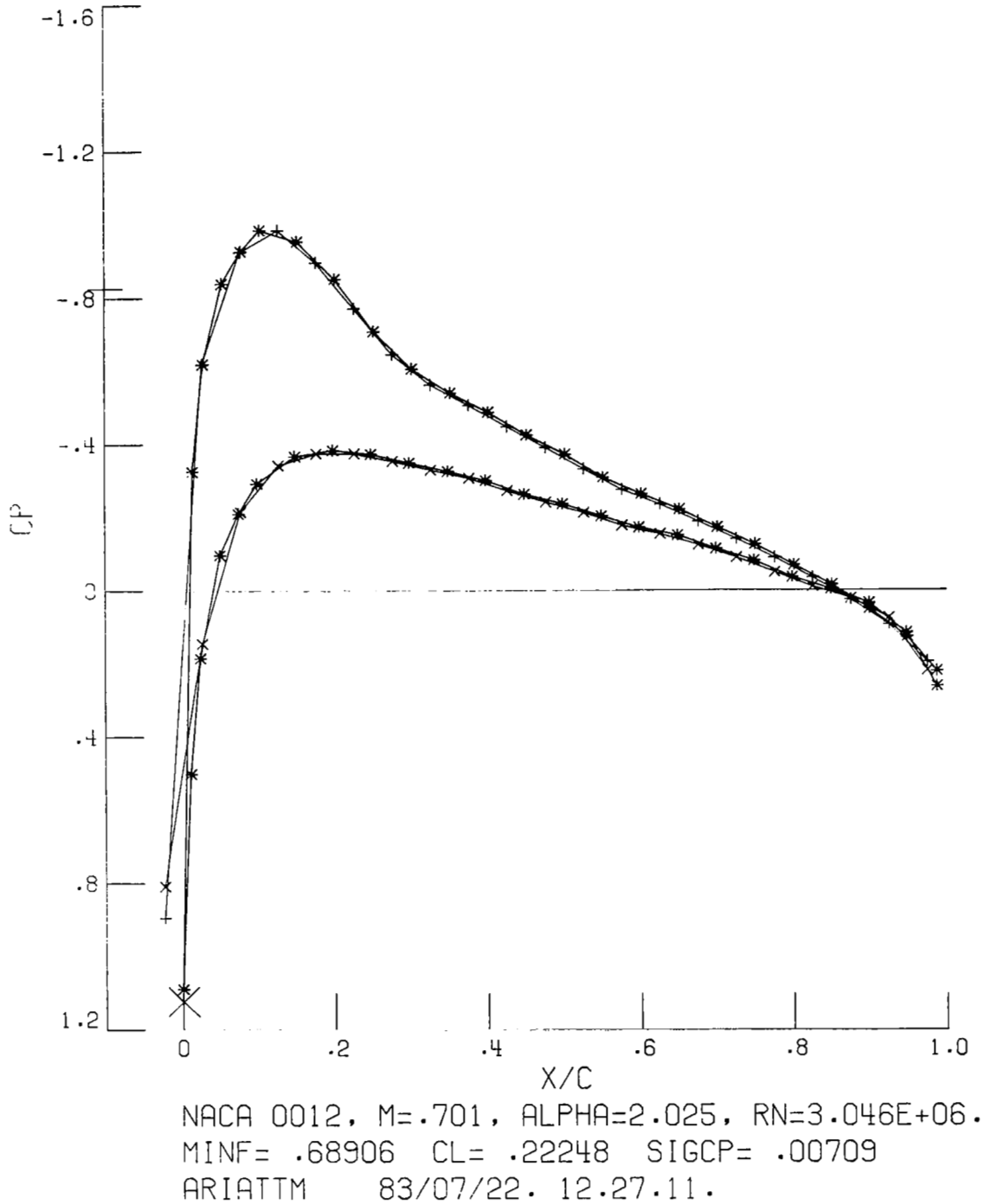

Figure 3.- Second frame of plotted output for sample case.

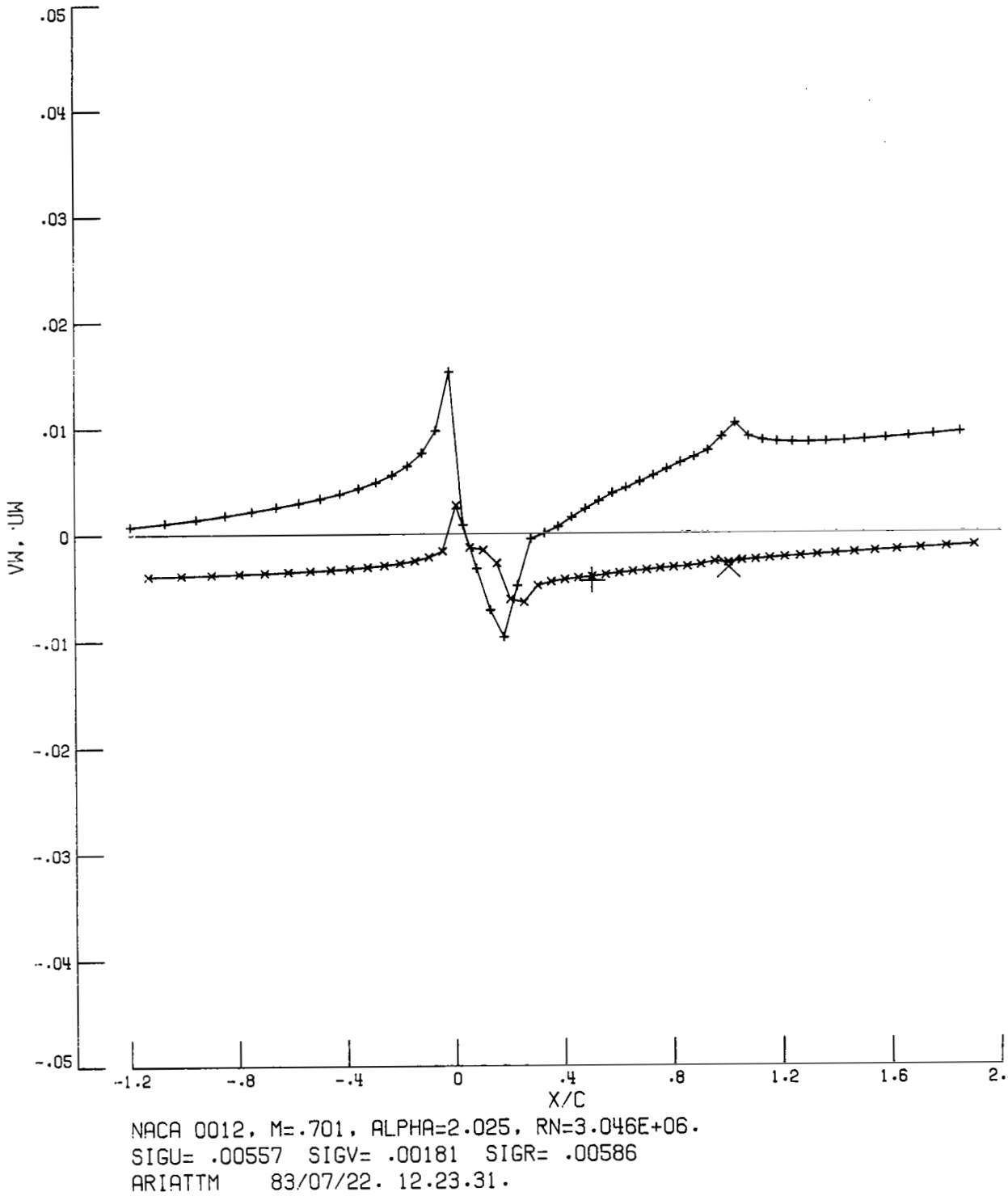

Figure 4. First frame of plotted output from unified procedure using sample case data.

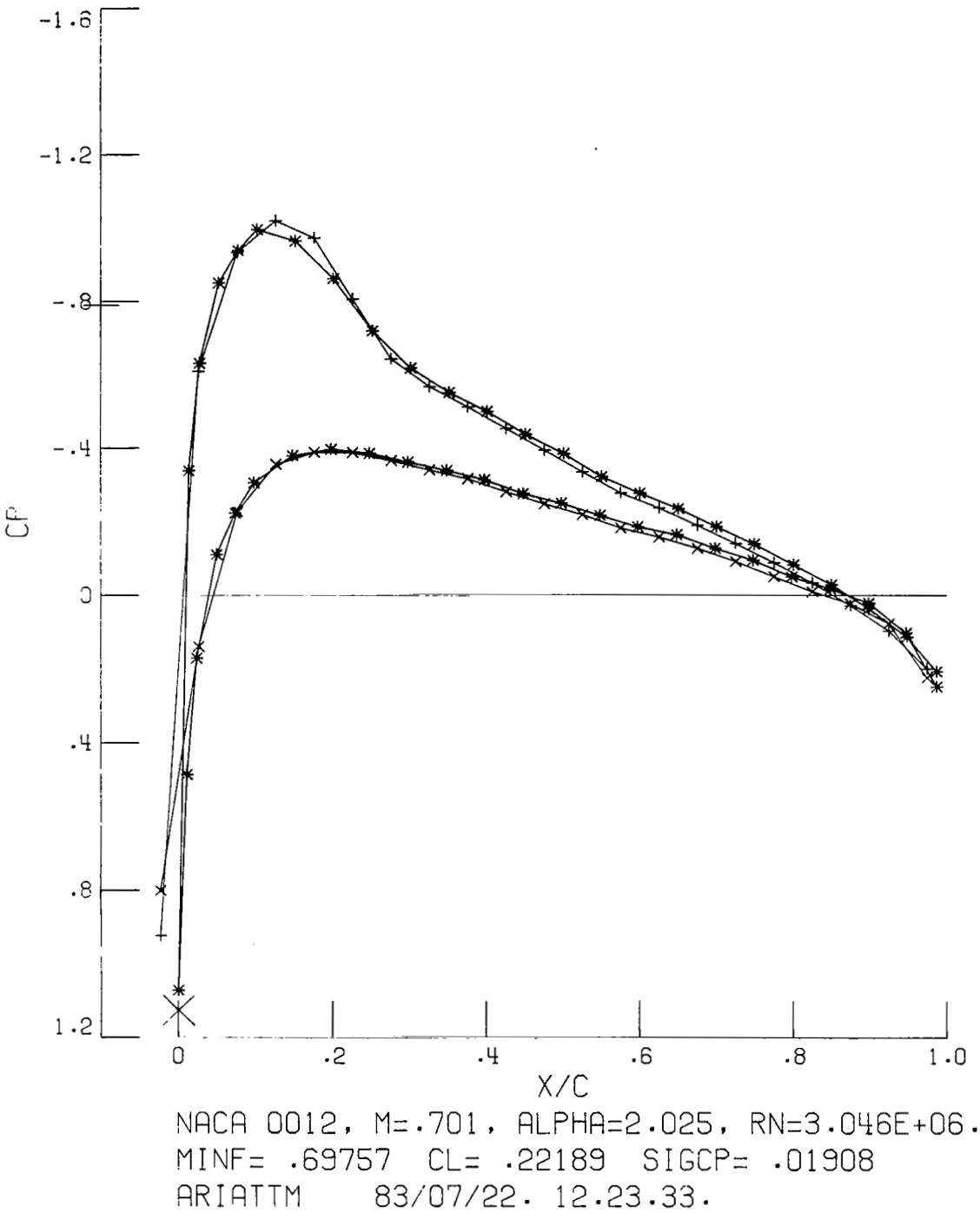

Figure 5.- Second frame of plotted output from unified procedure using sample case data.

1. Report No.	2. Government Accession No.	3. Recipient's Catalog No.
NASA CR-3777		

4. Title and Subtitle	5. Report Date
TWINTN4: A PROGRAM FOR TRANSONIC FOUR-WALL INTERFERENCE ASSESSMENT IN TWO-DIMENSIONAL WIND TUNNELS	February 1984
	6. Performing Organization Code
7. Author(s) William B. Kemp, Jr.	8. Performing Organization Report No.
	10. Work Unit No.
9. Performing Organization Name and Address Virginia Associated Research Campus 12070 Jefferson Avenue Newport News, VA 23606	11. Contract or Grant No. Cooperative Agreement NCC1-69
	13. Type of Report and Period Covered Contractor Report
12. Sponsoring Agency Name and Address National Aeronautics and Space Administration Washington, DC 20546	14. Sponsoring Agency Code

15. Supplementary Notes

Langley Technical Monitor: Jerry B. Adcock

16. Abstract

A method for assessing the wall interference in transonic two-dimensional wind tunnel tests including the effects of the tunnel sidewall boundary layer has been developed and implemented in a computer program named TWINTN4. The method involves three successive solutions of the transonic small disturbance potential equation to define the wind tunnel flow, the equivalent free air flow around the model, and the perturbation attributable to the model. Required input includes pressure distributions on the model and along the top and bottom tunnel walls which are used as bounda conditions for the wind tunnel flow. The wall-induced perturbation field is determined as the difference between the perturbation in the tunnel flow solution and the perturbation attributable to the model. The methodology used in the program is described and detailed descriptions of the computer program input and output are presented. Input and output for a sample case are given in an appendix.

17. Key Words (Suggested by Author(s))	18. Distribution Statement
Wall interference Wind tunnel corrections Sidewall boundary layer Transonic flow	Unclassified - Unlimited Subject Category 09

19. Security Classif. (of this report)	20. Security Classif. (of this page)	21. No. of Pages	22. Price
Unclassified	Unclassified	48	A03

For sale by the National Technical Information Service, Springfield, Virginia 22161

NASA-Langley, 1